Science of the Total Environment 774 (2021) 145676

Contents lists available at ScienceDirect

Science of the Total Environment

journal homepage: www.elsevier.com/locate/scitotenv

Review

Engineered algal biochar for contaminant remediation and electrochemical applications

Asha Singh [a], Rozi Sharma [b], Deepak Pant [c], Piyush Malaviya [b,*]

[a] Government Degree College Bishnah, Jammu 181132, J&K, India
[b] Department of Environmental Sciences, University of Jammu, Jammu 180006, J&K, India
[c] Separation and Conversion Technology, Flemish Institute for Technological Research (VITO), Boeretang 200, 2400 Mol, Belgium

HIGHLIGHTS

- Engineered biochars derived from pristine biochar modifications
- Various modification procedures for developing engineered biochars
- Recent advancements in engineered algal biochar vis-à-vis contaminant remediation
- Development of bioelectrochemical systems using algal biochar

GRAPHICAL ABSTRACT

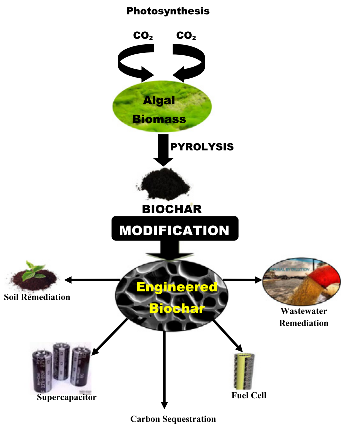

ARTICLE INFO

Article history:
Received 27 September 2020
Received in revised form 26 January 2021
Accepted 2 February 2021
Available online 6 February 2021

Editor: Yifeng Zhang

Keywords:
Algal biochar
Bioremediation
Engineered biochar
Resource recovery
Wastewater

ABSTRACT

Biochar, a pyrogenic black carbon is derived by pyrolysis of carbon-rich biomass in an oxygen-limited environment. The physico-chemical characteristics of biochar strongly impact the multifunctional role of biochar e.g., carbon sequestration and enhancement of soil fertility, biosorption or environmental remediation, fuel cells, supercapacitors, and biocatalyst. Owing to the poor performance of pristine biochar, engineered biochars have emerged, that are derived from physical, chemical, and biological modifications of pristine biochar to improve its surface properties and thus adsorption capacity. In the past two decades, researchers have been focussing more on low-cost biomass. Algal biomass is one such source that has shown significant prospective for biochar fabrication. The present review summarizes various applications of biochar, mechanisms associated with metal removal by biochar, various modification procedures for developing engineered biochars, algal biochar production methods as well as characterization of algal biochar. The review is intended to evaluate recent advancements and research in engineered algal biochar with a primary focus on contaminant remediation and the development of bioelectrochemical systems using algal biochar. This review opens new vistas and adds innovative ideas for future research utilizing engineered algal biochar, towards renewable, sustainable, and low-cost production of biosorbents for remediation of contaminated aqueous environments.

---

* Corresponding author.
E-mail addresses: piyushmalaviya@rediffmail.com, piyushmalaviya@jammuuniversity.ac.in (P. Malaviya).

https://doi.org/10.1016/j.scitotenv.2021.145676
0048-9697/

Contents

---

1. Introduction

Incessant urbanization and industrialization have resulted in the development model of "high energy consumption, high emissions, and high pollution" triggering ever-growing environmental concerns. Huge amounts of industrial effluents containing heavy metals remain a disquieting global environmental problem because of their toxicity, nonbiodegradability, and even the risk of biomagnification through the food chain (H. Wang et al., 2015).

To meet the EPA standards, various treatment approaches have been applied for removing numerous heavy metals from industrial effluents viz. coagulation, electrochemical methods, flocculation, ion exchange, precipitation, and membrane-related processes viz. ultrafiltration, nanofiltration, etc. (Llanos et al., 2010; Malaviya and Singh, 2011), however, most of these technologies have some shortcomings. The use of expensive chemicals is a prerequisite in some of these methods in addition to the huge quantity of toxic sludge generation and high energy requirement (Wang and Chen, 2009). Consequently, finding new, green, and cost-effective technologies is vital for the remediation of different pollutants from aquatic matrices that will diminish these drawbacks (Malaviya and Singh, 2016; Singh et al., 2016; Malaviya et al., 2020).

Discussions on sustainability, budding non-exhaustible resources, and potential green infrastructure technologies present an area of research focus in recent years (Tiquia-Arashiro and Pant, 2020; Sharma and Malaviya, 2021). Biosorption of heavy metals and other pollutants, using natural substances of biological origin become a promising substitute for conventional treatment technologies, which offers an ecologically benign, economic, and efficient option to eliminate pollutants from industrial wastewaters (Singh and Malaviya, 2019). In comparison with different physico-chemical treatment methods, biosorption can be contemplated as a quick, reversible, cost-effective, and eco-friendly means for the reduction of environmental pollution (Vijayaraghavan and Balasubramanian, 2015). Novel adsorbents with high adsorption capacity have been developed in recent times with great efforts. However, the use of these biosorbents is still restricted in practical application.

In absence of oxygen or hypoxic conditions, thermochemical pyrolysis results in biochar production. Biochar has gained attention for its eco-friendly nature, cost-effectiveness, and high efficiency for contaminant remediation (Dawood et al., 2017). The word “biochar” is a combination of two words “bio” meaning “biomass” and “char” meaning “charcoal”. Biochar is characterized by a large specific surface area, spongy structure, along with abundant functional groups (like carboxylic, carbonyl, ester, hydroxyl, phenolic, pyridine-N, pyrrole-N, quaternary-N), which makes it an apt adsorbent for contaminant remediation from wastewaters (Zhu et al., 2018). Currently, many raw materials have been used for biochar preparation, such as bamboos (Fan et al., 2010); wood (Vaughn et al., 2013); safflower seeds (Angın, 2013); pine-wood (S.S. Wang et al., 2015); rice straw (Qian et al., 2017), sawdust (Zhou et al., 2017) and various other lignocellulosic plant materials (Sun et al., 2020). Biochar is a renewable resource and is an ideal resource for the treatment of wastewaters owing to its environmental as well as economic benefits. However, finding economical biomaterials with an advanced performance of biochar is a great challenge in wastewater remediation (Inyang et al., 2016).

In recent times, scientists and environmental engineers are exploring renewable and sustainable technologies all over the world, and in this context, aquatic biomass has attained significant attention being an environment-friendly and rich source of energy (Abbasi and Abbasi, 2010). Algal biomass is mainly exploited for producing renewable energy sources (Sevda et al., 2019) and treatment of wastewaters (Mishra et al., 2019). Although, some brief reviews linked to the production and characterization of algal biochar are available (K.L. Yu et al., 2017a; Chen et al., 2020), however, a comprehensive study regarding different aspects of algal biochar for contaminant remediation is still lacking. In this context, the present review provides an insightful discussion regarding production strategies, characteristics, modifications, and remediation potential of algal biochar for inorganic and organic contaminants along with its associated mechanisms. Additionally, the application of biochar with potentially enhanced electroactive properties (e-biochar) for contaminant remediation is also discussed separately. Therefore, this review critically synthesizes state-of-the-art advancements and innovations in the adsorption of various contaminants by algal biochar.

2. Biochar

A porous and carbon-containing organic solid material having strong anti-decomposition properties and a high degree of aromatization, produced during pyrolysis of lignocellulosic biomass under poor oxygen conditions is known as biochar. It finds its application in environmental remediation for the elimination or reduction of noxious heavy metals, dyes, antibiotics, and other organic and inorganic pollutants from aquatic environments (Ahmad et al., 2014; Inyang et al., 2016). Biochar, a novel adsorbent, is also used to improve environmental and agricultural sustainability as well as that of energy. The mounting interest in biochar has further induced researches in multidisciplinary areas of science and engineering aspects. Pyrolytic biochar enhances soil fertility and owing to its chemical stability, also mitigates global warming by acting as a long-lasting sink of atmospheric carbon dioxide. Advantage of developing biochar for mitigating global warming (Koga et al., 2017), as a soil amendment (Liu et al., 2018), producing bioenergy (Field et al., 2013), and for the treatment of wastes (Mohan et al., 2014a) has been displayed in many studies.

In the last decade, a significant rise in research on biochar has been observed that can be evaluated by further publications on the same. Various publications conducted recently have confirmed the biochar's tremendous capacity to manage and control the toxicity of different organic compounds in soil and aqueous systems viz. hydrophobic organic compounds, pesticides and antibiotics, and many inorganic pollutants (Inyang et al., 2014; Lattao et al., 2014; Meng et al., 2014; Mohan et al., 2014b; Rajapaksha et al., 2014).

Biochar can be prepared by thermal pyrolysis of almost all kinds of biomass. However, biochar made from waste biomass is comparatively eco-friendly and more cost-effective as suggested by the life cycle assessment of pyrolysis-biochar systems (Cowie et al., 2012). Biochar elemental composition reflects almost the original composition of raw biomass from which the biochar is prepared which also determines its physical characteristics (Laine et al., 1991). Biochar properties are controlled by temperature and type of feedstock; like pH, recalcitrance, volatile matter and yield depend on temperature while C content, cation exchange capacity (CEC), carbon storage capability, mineral composition, and ash content are governed by the latter (Zhao et al., 2013).

Innate properties of biochar determine its utility for particular environmental applications, for instance, biochar with the larger specific surface area are used as sorbent material and those with higher recalcitrance are used for carbon-sequestration (Zimmerman, 2010). Biochars having better water holding capacity (WHC) and a large concentration of nutrients and minerals can be successfully applied to soil as amendments (Graber et al., 2010) and improve its fertility. Thus, engineered biochar can be potentially utilized for diverse applications including carbon sequestration, environmental remediation, as a catalyst for biofuel production, waste recycling, and energy storage (Tan et al., 2017) (Fig. 1) all of which are discussed below.

2.1. Environmental remediation using biochars

2.1.1. Water treatment

Biochars can efficiently adsorb heavy metal ions like As(III), As(V), Pb^{2+}, Hg^{2+}, Cd^{2+}, Cu^{2+}, Cr(VI) and other inorganic pollutants viz. phosphate and nitrate from the aquatic environment (Zhang and Gao, 2013; Xue et al., 2016). Biochar's properties viz. greater surface area, degradation resistance, and negative charge makes it an excellent adsorbent and thus, provide sustainable means to remove phenolics, halogenated compounds, polar organic molecules, and various cations from wastewaters via complexation, electrostatic interactions, ion-exchange, precipitation, and different sorption methods (Tan et al., 2015; Sizmur et al., 2016).

2.1.2. Soil remediation

Biochars can stabilize different heavy metal ions in soil owing to their larger surface area, higher CEC, and the occurrence of oxygen-containing functional groups. Biochars reduce the bioavailability of these heavy metals to terrestrial floras and hence, the resultant toxicity is also reduced (Beesley et al., 2011; Park et al., 2011).

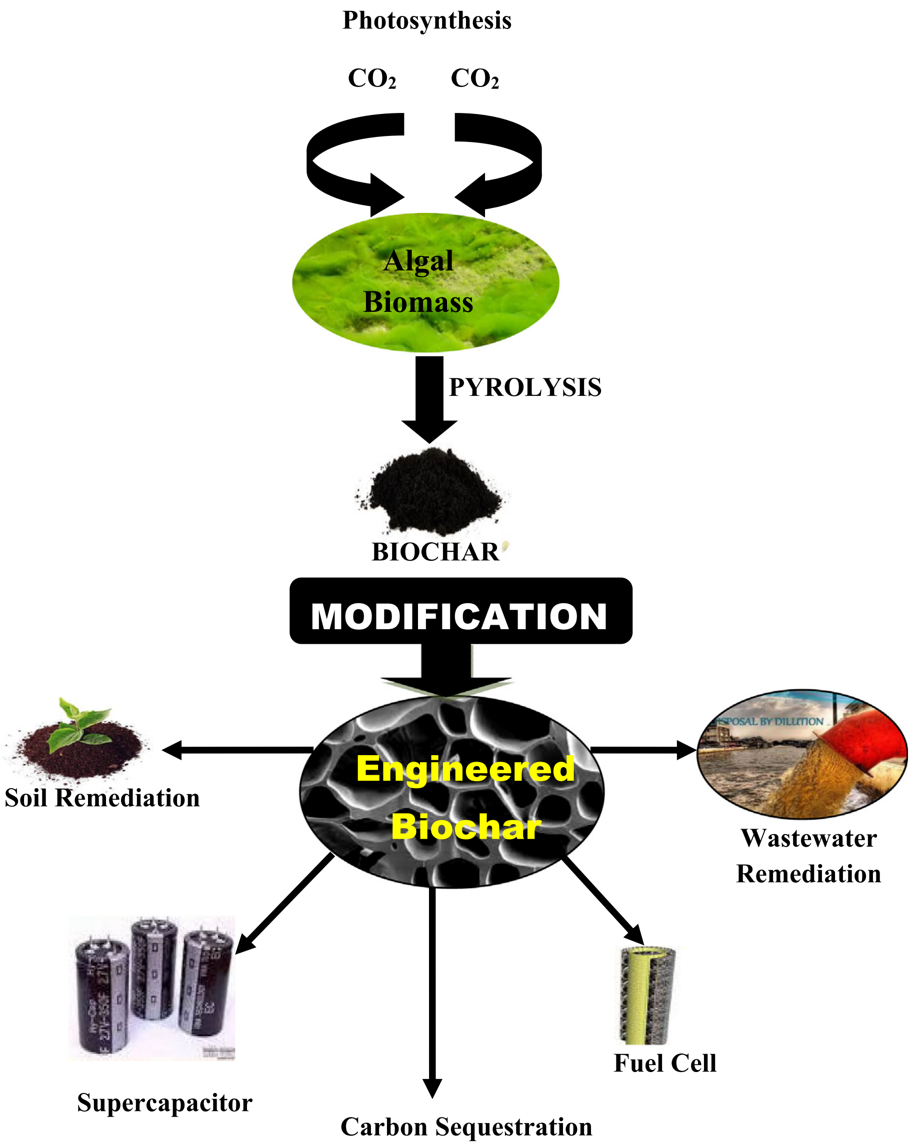

Fig. 1. Engineered algal biochar (EAB) for environmental sustainability.

2.2. Carbon sequestration

The role of biochars in mitigating climate change effects at a global scale has scientific recognition (Molina et al., 2009). The International Biochar Initiative credits biochar for its global warming mitigation potential as it absorbs approximately 3.67 Gt of CO_2 per year.

Approximately 12% of greenhouse gases can be potentially sequestered by biochars (Ennis et al., 2012). Biochars have long (>1000 years) residence time in soil that makes them a perfect tool for carbon sequestration (Liang et al., 2008).

2.3. Agricultural sustainability

2.3.1. Improvement in soil properties

Biochar significantly improves the WHC of soil, influences nutrient retention in soil, and affects nutrient cycling by indirectly affecting different biogeochemical mechanisms taking place in the soil (Liang et al., 2006; Abel et al., 2013). Biochar's WHC is ascribed to its highly porous nature, specific surface area, the occurrence of functional groups on its surface, and total pore volume (Mohamed et al., 2016). Crop productivity can be increased by applying biochar integrated with fertilizers or different types of compost in fields. The addition of biochar changes or enhances different variables viz. soil pH, soil microfauna, carbon percentage, bulk density, nutrient holding capacity (NHC), CEC and WHC of soil, etc.

Application of biochar to soils may enhance the abundance of microorganisms, and thus alters the microbial community profile in a manner that both reduce the microbial diversity and selectively enrich specific taxa viz. bacterial, archaeal and fungal populations (Khodadad et al., 2011). Such alterations in the microbial community are the outcome of an additional supply of nutrients from the labile carbon of biochar. This adds to the fact that biochar facilitates the living conditions of the microorganisms and subsequently protects them from the grazers or competitors in biochar pores (Lehmann et al., 2011). Such environments favouring microbial growth may encourage the biodegradation of organic contaminants (Kong et al., 2014). Biochar affects the activity of microorganisms variably. The following mechanisms are reported that are classified as direct and indirect impacts (Zhu et al., 2017).

2.3.1.1. Direct impacts.

(1) With its pore structures and surfaces, biochar provides shelter for soil microorganisms (Quilliam et al., 2013).
(2) Biochar contains essential nutrients and ions adsorbed to its surface and these are essential for the growth of soil microorganisms (Joseph et al., 2013).

(3) Biochar is also known to trigger the potential toxicity associated with volatile organic compounds (VOCs) and persistent free radicals (Fang et al., 2014).

2.3.1.2. Indirect impacts.

(1) Improvement in soil properties essential for microbial growth (aeration, pH, and water content), thus, biochar positively alters the microbial habitats (Quilliam et al., 2013).
(2) Inducing variations in enzyme activities, impacting soil elemental cycles vis-à-vis microbial activities (Lehmann et al., 2011).
(3) Interruption in intra- and inter-specific communication between microorganisms via a combination of sorption and hydrolysis of signaling molecules (Gao et al., 2016).
(4) Biochar can also reduce soil contaminants through sorption and degradation, thereby protecting residing microbes from their toxic effects (Beesley et al., 2010).

Minerals, VOCs, and free radicals (Spokas et al., 2011) present in biochar can reshape the soil microbial community, influence microbial activity, and change the activity of soil enzymes. Soil enzymes catalyze various biogeochemical processes including elemental (N, P, and S) cycles and soil organic matter turnover (Paz-Ferreiro et al., 2014). Therefore, biochar impacts the edaphic processes potentially.

Certain compounds in biochar (viz. benzene, methoxy phenols, phenols, carboxylic acids, ketones, furans, and PAHs) and persistent free radicals (PFRs) (cyclopentadienyls, phenoxyls, phenols, and semiquinones) are known as microbial inhibitors (Truong et al., 2010; Spokas et al., 2011; Lyu et al., 2016; Ghidotti et al., 2017; Zhu et al., 2017). Free radicals can impede the metabolism of exogenous organic substrates, interfere with cytochrome P450s, decrease the cell membrane integrity, reduce the concentrations of cellular glutathione (GSH), glutathione peroxidase (GPx), and superoxide dismutase (SOD), and induce oxidative stress in the microbial cells. In response, free radicals (specially semiquinone) can then generate reactive oxygen species (ROS) like hydroxyl radicals (OH), superoxide radical anion (O_2^-), and hydrogen peroxide (H_2O_2) (Liao et al., 2014). The formation of ROSs then initiates Fenton reactions which can lead to DNA strand break and damage (Zhu et al., 2017). Mechanisms behind interactions between biochar and microbes need further research. Moreover, the environmental effects of biochar also need further experimental verification.

2.4. Energy storage

2.4.1. Supercapacitor

Biochar has also been exploited for the manufacture of supercapacitors (Cha et al., 2016; Zhao et al., 2016). Different studies report that supercapacitors containing carbon electrodes can be produced from biomass of different feedstocks like seaweed biopolymers (Raymundo-Pinero et al., 2006), banana fibers (Subramanian et al., 2007), coffee seeds (Rufford et al., 2008), cotton straw (Chen et al., 2013), etc. Modification conditions and carbon precursor controls electrochemical characteristics of biochar-based double-layer capacitors, and also affect their working efficiency, electrochemically active functional groups present on their surface, their large specific surface area, electrical conductivity, pore-size distribution (Koutcheiko and Vorontsov, 2013).

2.4.2. Fuel cell

Biochar based cathodes find application in fuel cell systems. The high reversible capacity and high-power charge and discharge potential of biochars can be attributed to their large specific surface area, good conductivity, and permeability. Owing to their high electrical conductivity, chemical stability, and improved mass transportability; many carbon-rich substances can act as cathode catalysts in fuel cells (Huggins et al., 2014; Yuan et al., 2014).

2.5. Catalyst

Biochar-based catalysts are more advantageous than other catalysts. Biochar contains abundant heterogeneous functional groups that act as catalysts during pyrolysis, and small amounts of inorganic metal minerals in its biomass that further affect the pyrolysis pathway (Shen et al., 2014; Cao et al., 2021). Alkaline and alkali earth metal ions in concurrence with functional groups (especially hydroxyl and aldehyde) can form a metal ion-water complex that induces dehydration reaction in pyrolysis. Seaweeds like *Enteromorpha clathrate* contain a high concentration of potassium and sodium due to their marine growth environmental conditions, which provide a bonus advantage for the preparation of highly effective biochar-catalysts from them (C. Chen et al., 2019). In context to the performance of biochar based catalysts, various studies have been conducted viz. Taghavi et al. (2018); C. Chen et al. (2019); Anto et al. (2021); Cao et al. (2021).

3. Mechanisms of contaminant removal in biochar

The heterogeneous surface of biochar makes the sorption processes feasible. Adsorption depends upon the nature of pollutants and the chemical characteristics of the biochar surface (Rosales et al., 2017). Removal mechanisms in biochar for heavy metal ions and organic contaminants are described in the below-mentioned subsections.

3.1. Metal removal mechanisms in biochar

Removal of heavy metal ions from wastewater by biochar can be achieved through various mechanisms like ion exchange, precipitation, complexation, electrostatic interaction, sorption (Fig. 2). Biochars have a uniformly distributed network of pores including micropores (with diameter < 2 nm), mesopores (2–50 nm), and macropores (>50 nm), and this distinguishing feature of the char helps heavy metals to be physically sorbed onto them (Kumar et al., 2011; Mukherjee et al., 2011). Metal pollutants can be removed through various processes like electrostatic attractions in which negative charges on surfaces of biochars bind positively charged metal ions with them, and complexation in which ligands and functional groups present on biochar surface form complexes by interacting with various metals (Niu et al., 2017).

3.1.1. Physical sorption

It is a simple phenomenon that involves the diffusion of ionic forms of heavy metals into pores of sorbent biochar and thus, removes toxic ions easily without forming chemical bonds even.

3.1.2. Ion exchange

The mechanism in which protons and cations present on biochar surfaces are exchanged with heavy metal ions dissolved in aqueous solutions is named ion exchange. Various functional groups like carboxylic, hydroxylic, phenolic groups present on biochar surfaces facilitate chemical sorption and ion exchange (Liang et al., 2006). CEC is conferred to biochars by all these functional groups, subjected to the nature of feedstock and temperature at which pyrolysis is carried out. The maximum of CEC is observed between 350 and 400 °C which is probably because oxygenated functional groups are lost above 400 °C. Release of Ca, Mg, Na, K (base cations) from biochar influences the rate of chemical sorption of cations into biochar (Uchimiya et al., 2010).

3.1.3. Electrostatic interactions

Interactions between protons and cations present in an aqueous phase and delocalised electron cloud concomitant with aromatic groups present on the surface of carbon-rich biochars are termed electrostatic interactions. Electrostatic interactions are simply the interactions between C=C aromatic bonds and cation-π and C=C (Harvey et al., 2011). Graphene structures are formed in biochars at high temperatures

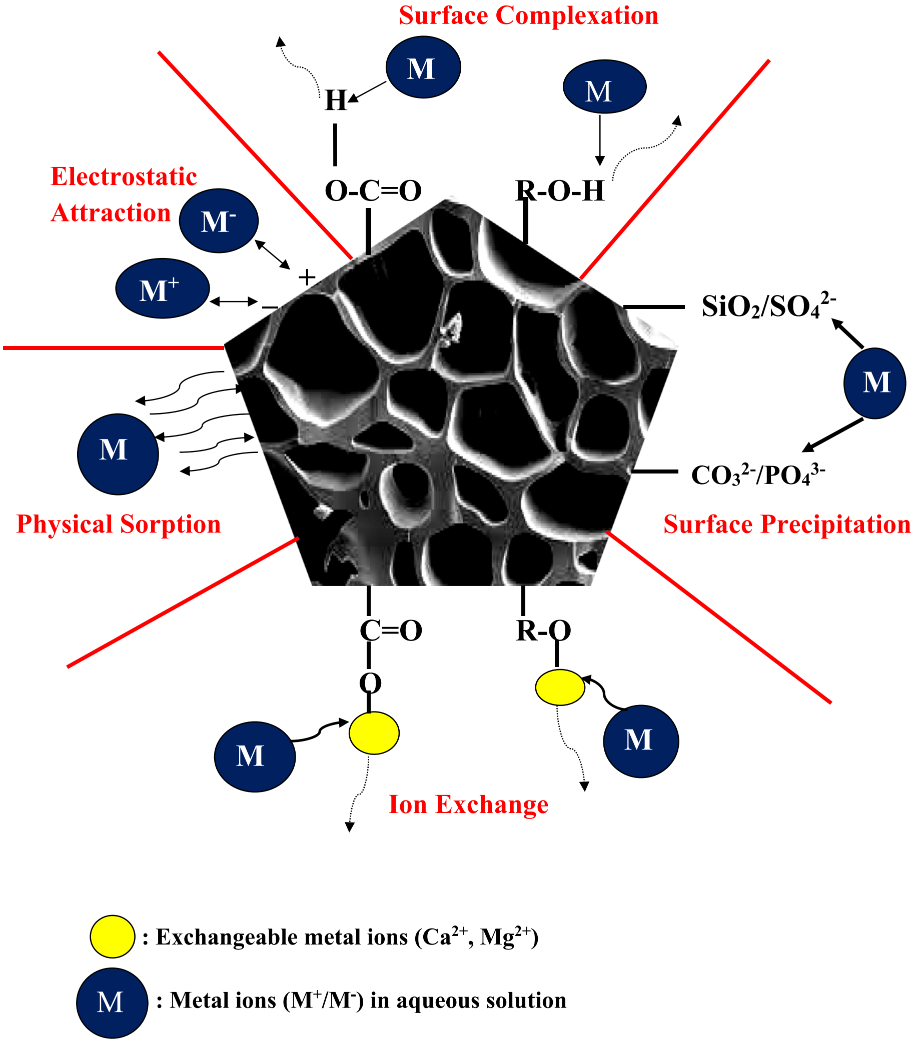

Fig. 2. Mechanisms for metal removal by biochar.

(>400 °C) that further favors electrostatic attractions (Keiluweit and Kleber, 2009).

3.1.4. Complexation

This mechanism involves multiatomic structure formations due to interactions between ligands and specific metal ions. Complexation is simply a binding mechanism that mainly removes those heavy metal ions that have a high affinity for ligands because of the presence of partially filled d-orbitals in their structure (Crabtree, 2009). Carboxylic, phenolic, and lactonic are the principal functional groups in biochars that are produced at low temperatures and form complexes with metal ions (Liu and Zhang, 2009).

3.1.5. Precipitation

The process of formation of solid complexes during sorption, in an aqueous solution or on the biochar surface is called precipitation. Rare earth elements and those metal ions that have ionization potential values between 2.5 and 9.5 can be precipitated out on biochar surface, comparatively more easily than other elements. Alkaline biochars are produced by thermal degradation of the plants containing cellulose and hemicellulose, at a temperature >300 °C (Cao and Harris, 2010). Since biochars cause a rise in solution pH, this can cause precipitation of metal oxides/hydroxides. For instance, digested bagasse biochar (with pH 10.93) can separate Pb from solutions by forming hydrocerussite $[(Pb_3(CO_3)_2(OH)_2)]$ precipitates on biochar surface (Inyang et al., 2011). Gurav et al. (2021) reported that certain mechanisms like electrostatic-interaction, hydrogen-bonding, ion-exchange, and metal-complexation govern the adsorption of red 120 dye by biochar prepared from biomass of macroalgae *Eucheuma spinosum*.

3.2. Removal mechanisms for organic pollutants in biochar

The major adsorption routes for organic contaminants are the physical route, precipitation route, and pore-filling route (Pignatello, 2011; Enaime et al., 2020). In the physical route, adsorbate settles down on the surface of the adsorbent, while in the precipitation route, the adsorbate form layers on the adsorbent's surface and condensation of adsorbate into the pores of adsorbent occur in the pore-filling route. Adsorption is facilitated by coulombic interactions, hydrogen bonding, π-interactions, dipole interactions, and hydrophobic interactions (Fig. 3; Tong et al., 2019). All these mechanisms are discussed in the below-mentioned subsections.

3.2.1. Covalent bonding

Covalent bonding that occurs through shared electron pairs is an irreversible sorption process and stronger than non-covalent intermolecular forces (Tong et al., 2019). The functioning of carbon-containing

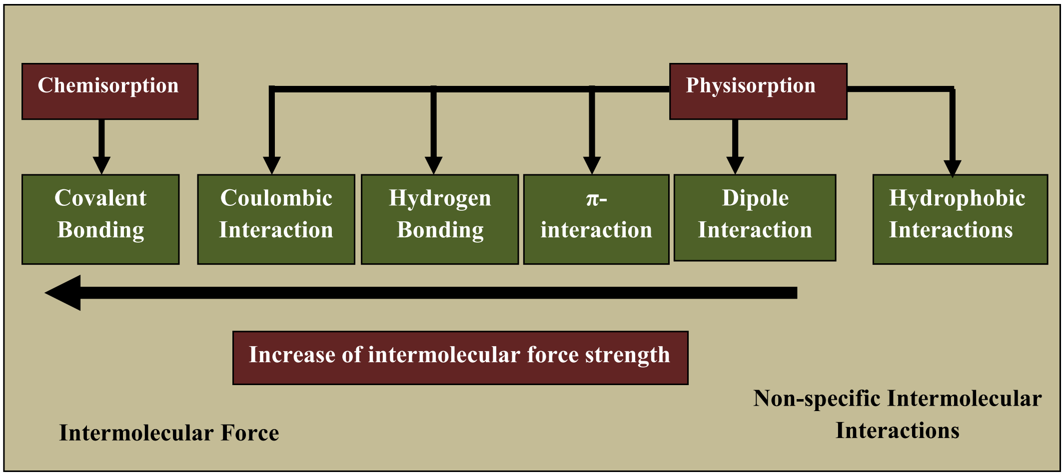

Fig. 3. Biochar-based remediation mechanisms for organic contaminants (modified from Tong et al., 2019).

biochar is achieved via free radical chemistry, and amidation, carboxylation, and fluorination reactions (Yang and Xing, 2010).

3.2.2. Coulombic interaction

Coulombic interactions exist in aquatic solutions between oppositely charged adsorbate and adsorbent. These interactions correspond to separable functional groups of organic compounds (adsorbate) and sorption on biochar's surface (adsorbent). Water pH and ionic strength influence the dissociation of functional groups for adsorption in an aqueous medium (Tong et al., 2019).

3.2.3. Hydrogen bonding

Hydrogen-bonding is a strong dipole interaction between hydrogen donor and acceptor. Hydrogen donor is bonded to nitrogen, oxygen, or fluorine atoms (acceptor) present within a functional group like —NH_2, —OH, —COOH, and electron-rich π-systems, and this interaction is known as hydrogen-bond. Adsorption due to hydrogen-bonding is stimulated in response to electrostatic repulsion between biochar and organic compounds. Lack of hydrogen bonds between water and oxygen-containing functional groups makes the diffusion of non-polar pollutants into the hydrophobic sites more distinct (Ahmad et al., 2014). For instance, sludge-based biochar shows a high affinity towards atrazine's amino group due to the presence of hydroxyl groups (Zhang et al., 2015).

3.2.4. π-Interaction

π-Interaction is a weaker dipole attraction than hydrogen-bonding. These interactions mainly exist between electron-rich π-systems and neutral organic molecules. π-system is simply a functional group-containing π-bonds (like C═C double bonds, aromatic rings), a bond that forms when diffusive electron orbitals overlap. π-systems are attractive to other π-systems and polar molecules (Tong et al., 2019).

3.2.5. Other dipole interactions

Intermolecular forces including permanent dipole interactions, dipole-induced dipole interaction, and fluctuating dipoles are some other dipole interactions that are mainly found between adsorbent and adsorbates containing polar functional groups (Kah et al., 2017).

3.2.6. Hydrophobic interaction

Entropy-driven non-specific interactions occurring in water are known as hydrophobic interactions. These interactions occur when non-polar groups aggregate in water for reducing their contact with water molecules to a minimum. Soluble pollutants can precipitate on alkaline biochar surfaces or get attach to biochars containing hydrophobic functional groups (Enamie et al., 2020).

3.2.7. Pore filling

Pore-filling is the sorption of organic pollutants into the pores of biochar. Pore-filling is influenced by total micropore and macropore volumes. The low ionic-radius of biochar adds to its adsorption capacity and promotes the penetration of contaminants into its structure (Rosales et al., 2017).

4. Algal biochar

Due to the discharge of environmental pollutants in the marine environment from different industrial activities, the excess macroalgal blooms have become a grave crisis in the coastal areas of the entire globe (Norouzi et al., 2017; Xiao et al., 2017). Consequently, considerable efforts have been made for using marine macroalgae as an energy crop (Safari et al., 2016). During pyrolysis of marine macro-algae, a huge quantity of carbon-rich porous solid is obtained (which is known as algal biochar) along with biofuels and other chemicals (Salimi et al., 2017). For biochar production, algal biomass is a suitable feedstock owing to its high growth rate and ability to tolerate varied climatic conditions thus, available at all seasons (Astals et al., 2015). Marine algae (like green tide algae) are more advantageous than those inhabited in freshwater owing to their much faster growth and capability to grow in saline water (Bird et al., 2011; Miao et al., 2012). The main reasons for selecting algae for preparing biochar are as follows:

(i) Algal biomass can be converted to biochar in just a few days owing to its thermochemical characteristic. Moreover, algae cultivation does not require vast lands (Xu et al., 2014; Lee et al., 2020).
(ii) Solid, liquid, as well as gaseous types of biofuels, can be recovered from algal biomass (Bird et al., 2011).
(iii) Their cultivation process is flexible, the growth rate is higher than terrestrial plants, and harvesting and processing stages are very simple (Neveux et al., 2014; Xu et al., 2014; Huang et al., 2017).

On processing of algae, lipid content generates biocrude, and pyrolysis of carbohydrates and protein-containing algal biomass yields biochar. Algal polysaccharides are also very useful (Lawton et al., 2013; Nagappan et al., 2019). The advantages and importance of algae biomass over terrestrial biomass is given in Table 1.

Table 1
Comparison of algal biomass with terrestrial biomass (Karthik et al., 2020).

Role	Algal biomass	Terrestrial biomass	Reference
Photosynthetic efficiency	6–8%	1.8–2.2%	Lee et al. (2020)
CO_2 fixation	High	Comparatively low	Lee et al. (2020)
Volatile matter	More	Less	K.L. Yu et al. (2017a, 2017b), S. Yu et al. (2017)
Farmland	Not necessary	Necessary	Xu et al. (2014)
Carbon capturing capabilities	High	Low	Yu et al. (2011)
Growth cycle	Shorter	Longer	Yu et al. (2011)

Algal biochar, owing to its unique physical and chemical properties, can be appropriately used in different research and practical applications. Particularly, based on their high specific surface area, oxygenated functional groups attached on their surfaces, hydrophilic character, porous surface, and low cost; algal biochars are a good substitute to some nanocarbon used in electrode materials (carbon nanotubes (CNTs) and graphene) (Gao et al., 2017; Pourhosseini et al., 2017). Mostly used microalgal species for biochar preparation are *Arthrospira platensis*, *Desmodesmus communis* (K.L. Yu et al., 2017a), *Dunaliella salina* (K.L. Yu et al., 2017b), *Nannochloropsis oculata* (Placido et al., 2019), etc. Among macroalgae, species mainly used are *Caulerpa taxifolia*, *Chaetomorpha indica*, *Chaetomorpha linum*, *Cladophora coelothrix*, *Cladophora patentiramea*, *Cladophora vagabunda* (Anto et al., 2021). Marine macroalgae are comparatively more useful in removing heavy metals (Poo et al., 2018). The specific surface area of marine macroalgae based biochars is 320 times lower than pinewood sawdust biochar but it is economically beneficial because this feature helps in higher yields of products. Furthermore, after pyrolysis, these macroalgae produce more biochar from the same amount of biomass than wood-derived materials which also add to economic viability. It is so because marine macroalgae contain lower lignin content which causes lesser volatilization and hence, lesser weight loss. Moreover, biochar prepared from *Saccharina japonica* has eleven times more removal efficiency for Cu^{2+}, twelve times higher for Cd^{2+}, and sixteen times greater for Zn^{2+} than biochar produced from pinewood sawdust (Poo et al., 2018).

Until now, limited literature is available on algal biochar and its environmental applications (Shukla et al., 2017). Algal biochars have comparatively high exchangeable nutrient content (N, P, K, Ca, Mg and Mo) than biochars produced from wood-based materials and thus, can add essential nutrients directly to soils (Bird et al., 2011). In general, algal biochars have high pH but low CEC, specific surface area, and carbon content (K.L. Yu et al., 2017b). Algal biochars with high pH values can neutralize acidified soils, and those with higher nutrient content containing nitrogen, inorganic elements, and ash can be utilized as a soil amendment (Kołtowski et al., 2017; Sun et al., 2017). Because of these advantages, algal biochar has been used as a fertilizer in agriculture in most of the studies (Torri et al., 2011) however; little consideration has been given to the adsorption potential of algal biochar.

Biochar prepared from algal biomass can perform better than lignocellulosic and wood-derived biochar when used as a soil amendment in mine rehabilitation projects (Bird et al., 2012). For instance, biochar prepared from macroalgae grown in wastewater under slow pyrolysis enhanced the yield of radish by 30–40% when added to poor quality soil (Roberts et al., 2015a).

Biochar produced from *Oedogonium*, freshwater macroalgae can be applied for the rehabilitation of ferrosol and sodosol (two types of stockpiled soil) from nearby coal mines and the growth of native plants in both the soils (Roberts et al., 2015b). Although algal biomass cultivated in wastewater has very high concentrations of few heavy metal ions, the biochar does not leach those metals into soil pore water-biochar mixture; instead, it contributes essential elements (particularly K) to water trapped in soil pores. Furthermore, biochars produced from several species of macroalgae at a pyrolytic temperature of 450 °C are characterized by high pH, presence of certain elements viz. C, H, N, TP, extractable nutrients (Ca, P, K, Na, Mg), and low carbon content, surface area, and CEC (Bird et al., 2011).

A hypothesis about the application of algal biochar as an adsorbent is postulated keeping in view that the algal cell wall comprises of many functional groups viz. hydroxyl, carboxylic, aldehydic, ketonic, phenolic, that serve as potential binding sites for adsorption of different pollutants (Nautiyal et al., 2016). High-quality biochar adsorbents can be produced by thermal pyrolysis of three freshwater algae viz. *Spirulina*, *Spirogyra*, and *Cladophora* (Chaiwong et al., 2012). Basic constituents of the biochar obtained from *Spirulina* sp. are similar to those of other algal biochars. However, carbon content was found to be higher in *Spirulina* sp. indicating that biochar from different species may have different properties (Chaiwong et al., 2013). Conversion of algal biomass into biochar, owing to all such advantages of algal biochar, is thus economically feasible in the field of biochar production (Bryant et al., 2012).

4.1. Production of algal biochar

By thermochemical conversions, viz. pyrolysis, hydrothermal carbonization, and torrefaction, algal biomass is transformed into biochar. Slow pyrolysis is the conventional process of synthesizing biochar that gives a higher yield of biochar. Hydrochar is a carbonaceous material produced by hydrothermal carbonization. Furthermore, a pre-treatment method viz. torrefaction can also convert living algal biomass into biochar, a carbonaceous solid fuel (Chen et al., 2015a; Kumar et al., 2017). Different methods employed for synthesizing algal biochar are explained in the following subheadings and are depicted in Fig. 4.

4.1.1. Pyrolysis

For converting biomass into important biofuels and biochars, the process of pyrolysis is considered one of the most potential technologies owing to its simplicity and speed. The pyrolysis process is classified into slow and fast or flash type, catalytic, hydrolytic, and microwave-assisted type on basis of differences in operating conditions. Biochar, bio-oil, and non-condensable biogases are mainly derived from microalgae pyrolysis (Sekar et al., 2021).

4.1.1.1. Conventional pyrolysis. The process of heating biomass in anaerobic conditions at a particular range of temperature around 300–700 °C is called pyrolysis and can be used for making microalgal biochar (Chen et al., 2015b). Slow, fast, and flash pyrolysis is based on the residence time of vapors, temperature, and heating rate (Lee et al., 2020). An increase in biochar production is observed with increased residence time, reduction in pyrolytic temperature, and low heating rate. Furthermore, the properties of raw biomass like moisture content and size of the particle also affect the biochar production via pyrolytic procedures (Tripathi et al., 2016). The maximum yield of biochar from different sources of biomass is obtained through slow pyrolysis than gasification methods and fast pyrolytic procedure (Mohan et al., 2014a). Through pyrolysis, approximately 50% carbon present in algal biomass can be contained in stable biochar (Bird et al., 2011).

Slow type pyrolysis is characterized by slow temperature increase and slow heating rate (ranging between 0.1 and 1 °C/s). A high amount of biochar and a smaller amount of liquid and gaseous products are mainly obtained after the termination of the process (Canabarro et al., 2013; Azizi et al., 2018). Biomass is decomposed at temperature intervals of 400–500 °C at different stages. Firstly, bonds break and moisture

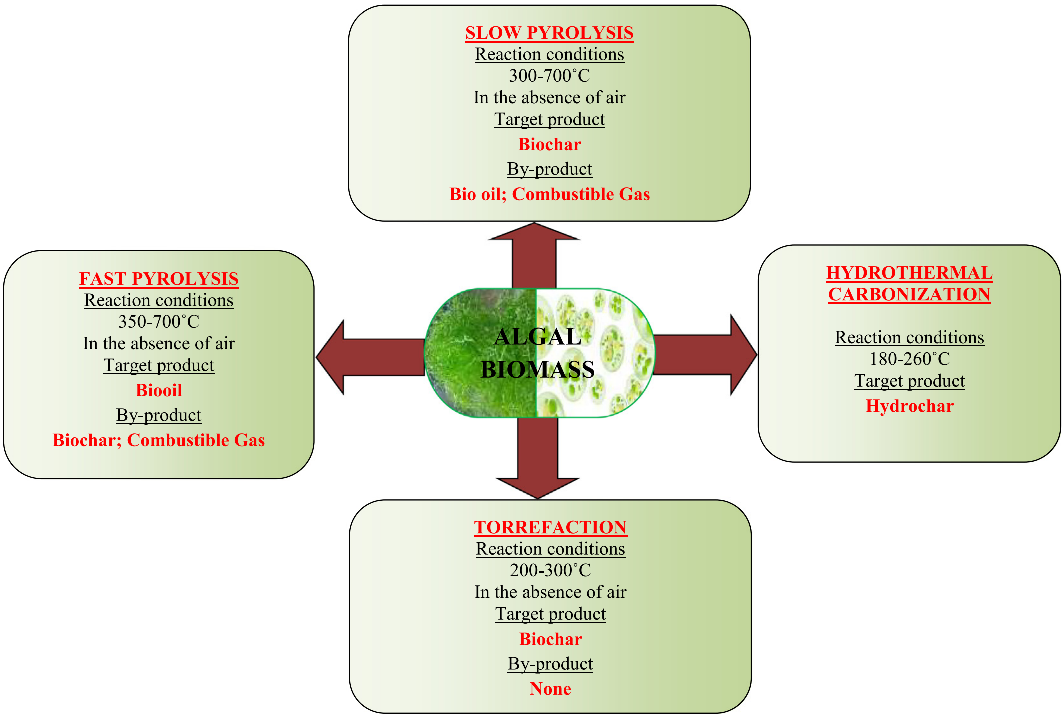

Fig. 4. Thermochemical conversion technologies for biochar production from algal biomass.

is removed; then carbohydrates, lipids, and proteins decompose; and at the final stage carbonaceous residues are formed. Various studies being conducted on biochar production from algal biomass through slow pyrolysis included Grierson et al. (2009), Bordoloi et al. (2016) and Akhtar et al. (2019). Widely studied microalgae are *Chaetoceros muelleri*, *Chlorella vulgaris*, *Dunaliella tertiolecta*, *Synechococcus*, and *Tetraselmis chui*.

Fast or flash type pyrolysis ensues at a very higher heating rate (of 1000 °C/s), lesser residence time, and a high transfer rate. The process is characterized by the rapid cooling of vapors formed during the process and >0.2 mm biomass particle size (Miao et al., 2004; Canabarro et al., 2013; Marcilla et al., 2013). This process produces 10–20% of gaseous products, 15–25% of biochar, and 60–75% of bio-oil (Andrade et al., 2018).

4.1.1.2. Microwave-assisted pyrolysis (MAP). In MAP, the heating source for pyrolysis is microwave irradiation, and operating temperature ranges between 400 and 800 °C. Microwaves are electromagnetic radiations in radio frequency ranging from 0.3 to 300 GHz, and wavelength ranging between 1 m to 1 mm.

Some of the benefits of this process are the high yield of biochar, low content of harmful chemicals in bio-oil, economic-feasibility, energy-saving, etc. The significant merit of MAP is speedy and uniform heating of large-sized biomass in a controlled way. Owing to high heating value, MAP yields comparatively more bio-syngas and bio-oil than the conventional type (Sekar et al., 2021). Application of MAP technique is still limited despite the above pluses because microwave irradiation is poorly absorbed. However, this drawback can be overcome by mixing algae with absorbers (like activated carbons, chars, metallic oxides) that will aid in achieving high temperature during MAP (Ellison et al., 2020). For example, Hong et al. (2017) carried MAP of *Chlorella*, *Porphyra*, and *Spirulina* at variable temperatures (400, 500, and 700 °C) in presence of catalyst SiC and model compounds (viz. cellulose and ovalbumin). L. Chen et al. (2019) used *Chlorella vulgaris*, added activated carbon and silicon carbide to it, and achieved an increased output of recoverable products.

4.1.2. Torrefaction

A thermochemical conversion process performed at a temperature range of 200–300 °C under atmospheric pressure in an anaerobic environment is called torrefaction (Chen et al., 2014a; Chen et al., 2015c). During torrefaction, a partially decomposed solid biomass with high carbon content called torrefied biomass or char is obtained. The process of torrefaction refers to thermal pre-treatment of biomass that leads to removal of volatiles through different decomposition reactions thereby upgrading biomass quality and alteration in its combustion behaviour as well (Nhuchhen et al., 2014).

Hydrothermal torrefaction/carbonization is the thermal pre-treatment process of torrefaction. There are further two types of this pre-treatment process: dry and wet (Chen et al., 2015a). Manufacturing of products with high energy-densification and that too within short residence time during wet torrefaction, owing to high rate of heat transfer in the liquid phase is an important advantage of this process (Coronella et al., 2012). Microalgae treated under hot compressed water during wet torrefaction can produce a solid product with high calorific value, lower ash content, and better hydrophobicity (Bach et al., 2017a). Approximately 62% of energy still retains in microalgae biomass even after wet torrefaction (Bach et al., 2017b). During the wet process, also the calorific value intensifies up to 21% and ash content reduces. The yield of biochar can be enhanced by carrying out torrefaction at low temperature and heating rate for short residence time (Nhuchhen et al., 2014).

Effect of range of torrefaction temperature on yields of solid, liquid, and gaseous components of *Laminaria japonica* reveals that an increase in temperature decreases solid yield due to decomposition of alginate and mannitol present in the plant, and increases liquid and gaseous yield (Uemura et al., 2015).

A solid yield of 51.3–93.9% can be achieved in the microalgae residue after torrefaction at 200–300 °C and residence time between 15 min to 1 h (Chen et al., 2016). A yield of 50.8–95.7% in solid components of torrefied microalgae *Chlamydomonas* sp. JSC4 residue can be accomplished, if the process occurs at 200–300 °C for 15–60 min (Mwangi et al., 2015). Thus, it is suggested that an optimum temperature of

≤250 °C is appropriate for torrefaction of microalgae residue with supplementary benefits like high energy-densification with less weight-loss. Isothermal and non-isothermal torrefaction characteristics also affect the features of *Scenedesmus obliquus* CNW-N (Chen et al., 2014b).

4.1.3. Hydrothermal carbonization (HTC)

An eco-friendly and economically-feasible thermochemical technique i.e., HTC has gained much attention in recent times (Erlach et al., 2012; Xiao et al., 2012). Hydrothermal carbonization is the production of carbon-rich biochar from carbohydrate components of biomass, a process being carried out at lower temperatures (180–260 °C) and elevated water pressures. The biochars thus produced are called hydrochar (Libra et al., 2011).

HTC process is more advantageous than the conventional carbonization process due to more products yielded towards the end of the process, and the low energy and time required for product formation (Tekin et al., 2014). Hydrochars differ from other chars in respect of their unique properties like uniform spherical particles, presence of functional groups (e.g., hydroxyl, carbonyl, carboxyl), electronic properties, and controlled porosity (Titirici et al., 2012). Microalgal hydrochar is also unique in its composition and is comparable to bituminous coal (Heilmann et al., 2010). Usually, biochar from the hydrothermal liquefaction is very porous due to the volatilization of organic matter from the feedstock, which consequently creates voids and ultimately leads to porous structure (Son et al., 2018).

In addition to the 3 techniques discussed above, there are other biomass transformation methods also including flash carbonization, laser, and plasma cracking technologies (Yang et al., 2019). These new technologies are less popular due to higher cost and energy consumption. Sol-gel, co-precipitation, solvothermal, succinylation are some additional methods that are adopted nowadays for biochar formation (Gupta et al., 2020). In the flash carbonization process, flash fire is ignited at a pressure of 1–2 MPa on an algae-packed bed, and biomass is then converted into biochar and other useful products (Cha et al., 2016). 40% of biomass is reported to be converted into biochar at 1 MPa (Mochidzuki et al., 2003). Laser pyrolysis is not widely applied (Metz et al., 2004) while plasma technique is applied in the generation of coke and syngas (Tang and Huang, 2005).

4.2. Characterization of algal biochar

Characterization of physico-chemical properties of biochar is necessary to determine the areas where it can be applied. The type and composition of algal biochar depend on certain factors like algal species, pyrolysis techniques, operating conditions, and activation methods (Chen et al., 2020). Biochar is generally alkaline whether derived from microalgae or macroalgae.

Differences exist between the properties of seaweed biochar and biochar produced from lignocellulosic biomass. For instance, biochar prepared from macroalgae exhibits properties like high nitrogen, hydrogen, and ash content, high electrical conductivity, low carbon content, and low cation-exchange capacity (Anto et al., 2021; Maddi et al., 2011). These properties are dissimilar to properties of biochar produced from lignocellulosic biomass (Table 2). Furthermore, differences also exist in terms of heating value which is higher for algal biochar than lignocellulosic biochar.

The yield of biochar and fixed carbon content is dependent on algal species. For example, for microalgae and macroalgae, biochar yield is 20–63% and 8.1–62.4%, respectively, and fixed carbon content is 4.9–29.10% and 1.7–27%, respectively (Karthik et al., 2020). The percentage of volatile matters produced by both types of algae is calculated as high as 44.80%. Ash content in macroalgae is twice the content present in microalgae. Ash contains elements like K, Ca, Na, Fe, Zn, Cu, and Mn (Lee et al., 2020). Moreover, macroalgae-based biochar has a greater porous structure in comparison to microalgae-based biochar because macroalgae have higher carbohydrates than microalgae (K.L. Yu et al., 2017b; Lee et al., 2020).

Usually, algal biochar has a small surface area but it increases on increasing the pyrolysis temperature (Bird et al., 2011). The pH range of macroalgae biochar rises from 7.6–13.7 to 8.7–3.7, when pyrolysis temperature increases. Biochar formed through hydrothermal carbonation contains numerous polar groups including oxygen-containing functional groups.

CEC measures the capacity of algal biochar to adsorb the cationic nutrients. A higher value of CEC of algal biochar is obtained by varying the pyrolysis temperature (K.L. Yu et al., 2017a). Various such properties of both macroalgae and microalgae-based biochars are discussed in the next sections.

4.2.1. Physical properties

4.2.1.1. Biochar yield. The biochar yield produced from microalgae and macroalgae ranges from 20 to 63% and 8.1–62.4%, respectively (K.L. Yu et al., 2017b). As pyrolysis temperature increases from 300 to 750 °C and residence time from 10 min to 1 h, biochar yield decreases. These differences in results are ascribed to differences in the chemical structure of feedstock biomass, in particular, that of their cell wall (Tag et al., 2016).

Biochar produced from *Cladophora glomerata* (at 550 °C) was reported to be 31% Chaiwong et al. (2012). In a study by Poo et al. (2018), an increase in temperature by 250, 400, 500, 600, and 700 °C led to a reduction in biochar yield by 47.1, 37.3, 31.5, 29.7, 25.9%, respectively when *Saccharina japonica* was put to pyrolysis, and 58.4, 44.6, 38.3, 35.0 and 32.8%, respectively in case of *Sargassum fusiforme*. This trend of decreasing biochar yield with increasing pyrolysis temperature was also reported in marine microalgae *Undaria pinnatifida* (Jung et al., 2016). Likewise, Michalak et al. (2019) also stated an inverse relation between algal biochar yield and temperature (63% for 300 °C and 47% for 450 °C). Furthermore, Gurav et al. (2021) also reported a 53.98, 45.56, 38.95, and 34.02% decline in yield of biochar prepared from *Eucheuma spinosum* when pyrolysis temperatures were increased by 300, 400, 500, and 600 °C, respectively.

At low temperature during pyrolysis, moisture and volatiles evaporate, de-polymerization occurs, and cellulose and hemicellulose content is fragmented. All this contributes to weight loss (Michalak et al., 2019; Yek et al., 2020).

4.2.1.2. Surface properties. In comparison to different lignocellulosic biomass, the surface area of algal biochar is low; however, it can be enhanced by increasing pyrolytic temperature (Bird et al., 2011). Macroalgal biochar derived from *Eucheuma* sp. has a significantly higher surface area (30.03–34.82 $m^2 g^{-1}$) in comparison to that of other species (1.29–8.87 $m^2 g^{-1}$) (Roberts et al., 2015c). Biochar particles derived from microalga, *Chlorella vulgaris*, were found to be compact and irregular, quite different from the feedstock structure (Wang et al., 2013). These results are similar to the results of Torri et al. (2011), where biochar was produced from *Chlamydomonas reinhardtii*. On the contrary, lignocellulosic based biochars normally retain their feedstock's structural properties.

When pyrolysis temperature increases from 600 to 800 °C; total pore volume, phosphate sorption capacity, and surface area of marine macroalgal biochar decreases which is ascribed to blockage of pore structures and their breakdown during pyrolysis (Paethanom and Yoshikawa, 2012; Jung et al., 2016). For instance, biochar that is produced from *Chlorella vulgaris* has a surface area (2.4 m^2 g) lesser than lignocellulosic-based biochar (Wang et al., 2013).

4.2.2. Chemical properties

4.2.2.1. Composition of inorganic elements. An abundance of inorganic elements has been reported in biochars derived from algal species. Carbon

Table 2
Physico-chemical characteristics of modified biochars produced from algal biomass in comparison to biochars produced from other biomass.

Biomass	Pyrolysis temperature	Volatile matter	Yield	Ash	pH	C	H	O	N	S	References
	°C	%	%	%		%	%	%	%	%	
Biochar from algal biomass											
Ulva sp.	450	–	–	42.6	10.0	22.6	1.2	–	2.7	–	Bird et al. (2010)
Cladophora coelothrix	450	–	–	32.1	8.72	34.6	1.5	–	3.3	–	
Cladophora patentiramea	450	–	–	47.0	9.12	20.3	1.2	–	1.7	–	
Chaetomorpha indica	450	–	–	73.5	7.83	10.2	1.2	–	1.1	–	
Chaetomorpha linum	450	–	–	16.0	9.61	23.6	1.3	–	2.4	–	
Cladophoropsis sp.	450	–	–	46.5	10.07	23.6	1.5	–	2.8	–	
Caulerpa taxifolia	450	–	–	20.9	9.65	21.8	1.2	–	2.4	–	
Cladophora vagabunda	450	–	–	54.2	9.87	21.8	1.2	–	2.0	–	
Chlorella sp.	630	68.4	25	7.8	–	10.1	–	–	–	–	Du et al. (2011)
Cladophora sp.	750	64.1	25	13.3	–	16.7	–	–	–	–	Maddi et al. (2011)
Lyngbya sp.	600	55.6	40	25.7	–	16.3	–	–	–	–	
Microcystis sp.	600		40	6.7	–	14.1	–	–	–	–	Miao et al. (2004)
Nannochloropsis	550	70.1	25	5.0	–	10.6	–	–	–	–	Borges et al. (2014)
Dunaliella tertiolecta	600	79.7	29	8.6	–	11.8	–	–	–	–	Francavilla et al. (2015)
Chlamydomonas reinhardtii	–	–	–	45	–	40	1.4	9.3	5.3		Bordoloi et al. (2016)
Scenedesmus dimorphus	–	–	–	39.6–44.2	–	46.8–53.2	7.9–8.5	31.4–39.5	5.6–6.5 -		
Rhizoclonium sp.	700	75.5	38	8.0	–	16.5	–	–	- -		Casoni et al. (2016)
Algae-dairy-manure slurry	500	–	–	33.56	10.07	46.96	2.47	48.44	1.68	0.45	Jin et al. (2016)
Vermiculite treated algal biochar	500	–	–	–	–	–	–	–	–	–	Wang et al. (2016)
Cladophora vagabunda	–	–	–	74.7	–	11.6	0.7	11.7	1.32		Huang et al. (2017)
Gracilaria sp.	–	–	–	43.2	–	30.9	2.2	16.5	2.8		
Saccharina japonica	500	–	–	–	11.29	62.3	2.1	31.3	2.7	1.6	Poo et al. (2018)
Sargassum fusiforme	500	–	–	–	8.01	64.9	2.2	28.4	2.4	2.1	
Spirulina	–	–	–	7.4		46.2	7.24	34.28	10.53		Simão et al. (2018)
Hijikia biomass	500	–	–	–	–	68.03	2.28	23.41	3.14	3.14	Son et al. (2018)
kelp biomass						64.35	2.05	27.46	3.07	3.07	
Brown macroalga	375	–	56.08	–	–	30.67	2.72	64.53	2.09	–	Choi et al. (2017)
Lipid extracted *Dunaliella tertiolecta* residues	–	–	–	–	–	60.8	4.7	14	11.4	0.2	Ryu et al. (2018)
Microalga residue	200–275	–	–	–	–	36.49	6.12	–	–	–	Zhang et al. (2018)
Cladophora glomerata	450	–	47	40.1	–	46.3	–	–	–	–	Michalak et al. (2019)
Chlorella	550	–	–	56.5	8.7	10.00	3.6	28.1	0.9	0.9	Amin et al. (2020)
High-salinity *Spirulina* residue	500	–	–	–	–	21.02		29.39	12.75	–	Tan et al. (2020)
Enteromorpha prolifera	400	–	45.75	42.77	4.5	50.51	4.48	37.75	6.38	0.87	H. Wang et al. (2020), Y. Wang
Magnetically modified *Enteromorpha*	400	–	66.29	22.93	4.68	45.36	3.06	46.58	4.12	0.89	et al. (2020), B. Wang et al. (2020)
Biochar from lignocellulosic biomass											
Dairy waste	600	–	–	–	10.0	65.42	0.68	–	3.63	–	Inyang et al. (2012)
Whole sugar beet	600	–	–	–	9.0	20.15	1.07	–	0.43	–	Inyang et al. (2012)
Peanut hull	100	–	–	–	–	64	–	–	2	0.14	Kastner et al. (2012)
Pine cone	500	–	–	2.1	4.0	71.2	3.0	20.4	0.5	–	Van Vinh et al. (2015)
Invasive plant	700	–	–	70.7	11.7	50.6	1.7	44.9	2.5	–	Rajapaksha et al., 2015
Pine cone	500	–	–	2.1	–	68	3.8	22	0.55	–	Van Vinh et al. (2015)
Zn-loaded pine cone	500	–	–	2.1	–	71	3.0	20	0.51	–	
Corn straw	600	–	–	10	–	85	1.8	5	0.80	–	Z. Yu et al. (2015)
Mn modified corn straw	600	–	–	12	–	73	0.33	11	0.72	–	
Sunflower seed hull	700	79.8	25	2.1	–	18.1	–	–	–	–	Casoni et al. (2016)
Rice husk	550	–	38.86	–	–	44.73	1.80	7.69	0.73	–	Zhang and Xiong (2016)
Biogas residue	700	–	0.20	58	–	29	0.96	59	1.3	–	Liu et al. (2016)
ZnCl2-activated biogas residue	700	–	7.5	78	–	34	1.0	43	1.8	–	
Corn stem	620	–	–	10	–	85	5.2	5	0.80	–	Lin et al. (2017)
Fe/Mn modified corn straw	620	–	–	18	–	67	2.4	7	1.8	–	
Pinewood sawdust	500		–	–	4.46	87.4	2.8	9.4	0.4	0.1	Poo et al. (2018)
Corn stalk	600	73.8	24	5.8	–	15	–	–	–	–	Muneer et al. (2019)
Coconut shell	500	71.5	31	1.3	–	19.3	–	–	–	–	Samsudin et al. (2019)
Coffee husk	350	–	39.82	–	–	69.96	3.63	–	3.58	0.24	Setter et al. (2020)

(C), Hydrogen (H), Nitrogen (N) and Sulphur (S) content present in algal biochar is 28.5%–59.2%, ~7%, 2.5%–11% and 0.5%–1.5%, respectively (Chen et al., 2020). For instance, biochars derived from lignocellulosic biomass contain lower concentrations of Ca, Mg, P, and K than algal biochar derived from *Chlorella vulgaris* (Wang et al., 2013) and high concentrations of N (0.3–2.8%), P (0.5–6.6 g/kg), and K (5.1–119 g/kg) are present in algal biochars derived from red and brown seaweeds (Roberts et al., 2015c).

4.2.2.2. pH. Macroalgal biochar shows the pH in the range 7.6–13.7, however, the literature on pH values of biochar derived from microalgae is scant. It was reported that values of biochar pH vary with the type of algae and pyrolysis temperature. For instance, the pH of biochar derived from algae (8.7–13.7) rises with an increase in the pyrolytic temperature (250–600 °C) (Tag et al., 2016). A rise in biochar pH is ascribed to a rise in relative ash content of biochar formed under severe pyrolysis. The pH of biochar is also correlated with oxygen-containing functional groups present on its surface (Ronsse et al., 2013). At lower temperatures (200–300 °C), cellulose decomposes and phenolic substances and organic acids are produced. While beyond 300 °C, alkali salts dissociate from organic matter which increases pH (Poo et al., 2018).

In a study led by Gurav et al. (2021) a rise in the pH of biochar prepared from biomass of macroalgae *Eucheuma spinosum* was observed from 3.93 at 300 °C to 11.8 at a higher pyrolysis temperature of 600 °C. Macroalgae BCs showing higher pH values at higher temperatures were attributed to exclusion of acidic functional groups, separation of alkali salts (such as Ca, K, Mg, Na, P), and retention of alkaline groups.

4.2.2.3. Cation exchange capacity (CEC). CEC of biochar shows its capacity for the adsorption of cation nutrients. Thus, biochar having high CEC is beneficial as it prevents leaching of nutrients in the soil. A negligible amount of Al and high concentrations of exchangeable cations (like Ca, Mg, Na, K) are present in biochar prepared from seaweed (Roberts et al., 2015c). In comparison to biochar derived from vine pruning and orange pomace, algal biochar shows higher values (25.6–52.6 cmol/kg) of CEC at different pyrolysis temperatures (Tag et al., 2016).

4.2.2.4. Types of functional groups. Spectral analysis of disrupted macromolecular crystal structure of algae by Fourier transform infrared spectroscopy (FTIR) identifies different functional groups present in it and its products like algal biochar and bio-oil produced after hydrothermal liquefaction (Biswas et al., 2017). Various oxygen-containing (—COOH, —OH, C═O) and nitrogen-containing (pyridine-N, pyrrole-N, graphitized-N, oxidized-N) functional groups are present in algal biochar (Chen et al., 2020).

4.3. Factors affecting algal biochar properties

Physico-chemical properties of algal biochar are determined by the pyrolytic procedure, the temperature at which the process occurs, chemical activation, residence time, heating rate, and reaction vessel (Mukome et al., 2013; Jindo et al., 2014). Biochar prepared from *C. vulgaris* at 450–600 °C has a higher concentration of C, H, and N in comparison to the biochar derived at low temperatures (Palanisamy et al., 2017). Seaweed can yield 84% biochar when pyrolyzed at 250 °C at a heating rate of 5 °C/min and holding time of 30 min (Tag et al., 2016).

There is a difference in the elemental composition of biochars derived from diverse macroalgae. For instance, red microalga has a greater proportion of sulphur and potassium and a lower fraction of carbon and hydrogen in biochars derived from them than those prepared from brown seaweeds. Furthermore, species collected from different locations also show variations in many physicochemical properties of the biochar derived from them, especially CEC. Differences in concentrations of exchangeable K in *Undaria* sp. and *Kappaphycus* sp. (ranges: 13–420 cmol/kg and 26–210 cmol/kg, respectively) are attributed to the location (Roberts et al., 2015c). Similarly, variations in yield and value of ash content of *Cladophora vagabunda* are also observed with varying locations (Bird et al., 2012).

Differences in biochar yield and properties are allied to the composition of the feedstock, processing technique, and pyrolyzing conditions. A mixture of algae (*Cladophora coelothrix*, *Chaetomorpha indica*, *Ulva flexuosa*) yields higher (74.5% on a dry weight basis) biochar than *Derbesia tenuissima* (8.1%) (K.L. Yu et al., 2017a).

Functional groups (especially oxygen (O)-containing) present at the surface of biochar changes with changing pyrolysis temperature. Carboxyl group in O-containing groups is important in typifying biochar (K.L. Yu et al., 2017a). For example, when marine algae are subjected to pyrolysis, cellulose present in it is changed to a carboxyl group or esters (oxygenated functional group). But when the temperature rises, carbonization of carboxyl groups occurs and oxygenated functional groups disappear (Poo et al., 2018). This may result in the decreased potential of biochar for heavy metal adsorption because active sites (i.e., carboxyl groups) are no more. Therefore, it is necessary to define suitable pyrolysis temperature at which O-containing functional groups exist in abundance.

Ge et al. (2020) while studying HSR (high-salinity *Spirulina* residue) derived biochar reported that when carbonization temperature increased from 350 to 700 °C and time rose from 90 to 540 min; aromaticity, porosity, and positive charge of biochar enhanced but O-containing functional groups and C—N bonds cracked. Moreover, sorption of Hg(II) was also decreased. Furthermore, Poo et al. (2018) reported that when pyrolysis temperature increased and carbonization proceeded, the honeycomb structure of macroalgae warped and pore size enlarged. Hammes et al. (2008) observed that above 900 °C, biochar walls deteriorated and the size of pores increased.

5. Engineered biochars

Biochars show numerous advantages, still, pristine biochars are not proficient in the removal of different pollutants and heavy metals owing to lower pore volume and lesser surface area. Consequently, it becomes very essential to improve this innovative material by activating it through various modifications. Biochar engineering deals with the creation of modified or activated biochar (Ok et al., 2015). Engineered biochar is derived from the physical, chemical, and biological modification of pristine biochar that improves its surface properties viz. porosity, pH, CEC, functional groups, specific surface area, and ultimately higher adsorption than basic pristine biochar (Mohamed et al., 2016; Rajapaksha et al., 2016).

Adsorption characteristics of engineered biochar are affected by pyrolysis temperature because when temperature changes; surface area, surface functional groups, distribution of pores, and mineral composition of the biochar also changes (Ahmad et al., 2012). Biochar produced between temperature ranges of 300–400 °C contains diversified aliphatic and cellulose structures and other organic characters (Novak et al., 2009) while biochars formed at high temperatures (600–700 °C) undergo dehydration and deoxygenation and thus left with only H and O functional groups in their structure, however, such biochars have well-organized carbon layers and highly aromatic characteristic (Uchimiya et al., 2011).

The yield of biochar declines by about 10% with a rise in pyrolysis temperature by 100 °C (Fletcher et al., 2014). Accordingly, higher pyrolysis temperatures produce biochars with less oxygenated functional groups, high pH, and higher concentrations of carbonates and base cations (including total, soluble and exchangeable) (Qian et al., 2013). Hence, by increasing the pyrolysis temperature, alkaline biochars capable of precipitating a maximum of metal cations are created (Kim et al., 2013).

Both O-containing and N-containing functional groups in algal biochar show significant properties for removing pollutants (Cho et al., 2013; Chen et al., 2017). Phenolic (—OH) and amino (—NHx) groups containing abundant unpaired electrons also play a vital role in removing pollutants. Moreover, the addition of N-functional groups and organic/inorganic N-precursors (NH_4Cl, urea, thiourea, NH_3) improves the alkalinity of biochar.

Ash of biochar comprises of metallic and non-metallic elements and its concentration ranges between 18.6%–58%. Inorganic element content increases with increasing pyrolysis temperature. Metal ions help in increasing CEC for the adsorption of heavy metals (Ho et al., 2017).

Different pyrolysis processes influence the characteristics of biochar differently. Thus, specifically ‘designed algal biochar’ is used for specific applications. Various physico-chemical and biological methods used for creating activated biochar include treatment of feedstock with different acids, bases, clay minerals, metal oxides, steams, biofilms, carbonaceous materials, etc. (Rajapaksha et al., 2016). Fig. 5 shows all those treatments that serve the purpose of increasing surface area and surface properties of biochar and using the surface of biochar as a platform for embedding additional materials/organisms having beneficial surface properties. Different modifications methods for biochar are described below.

5.1. Biological modification

Biochar produced from pretreated feedstocks by anaerobic digestion after biological engineering is indeed a biologically modified biochar (Yao et al., 2015; Yao et al., 2018). Pyrolysis and anaerobic digestion produce activated biochar with higher values of surface area, anion exchange capacity (AEC), CEC, and pH. Activated biochars are hydrophobic in nature and have a more negative charge on the surface in comparison to pristine biochars because biological modification leads to alterations in redox potential as well as pH of feedstock (Inyang et al., 2010). Owing to higher values of CEC and AEC, biologically activated biochar can be used as ion exchangers for sequestering both cations and anions from wastewater.

5.2. Physical activation

Physical modification of biochar comprises steam or gas (CO_2) activation, ball milling, magnetic and microwave modification. It is a two-step procedure in which biomass firstly undergoes charring through any thermochemical process and in the second step it activates to form a spongy structure (Anto et al., 2021). Activated biochar produced by physical modification leads to improvement of pore structure, the introduction of oxygenated functional groups, and is a clean method in comparison to chemical modification (Qian et al., 2015).

5.2.1. Steam

In steam activation, after the initial pyrolysis reaction, a second stage treatment of resulting biochar by subjecting it to partial gasification with steam is carried out. This process increases devolatilization and formation of crystalline C in the resulting activated biochar (Chia et al., 2015). Properties of biochar are changed after steam application due to the removal of the trapped products of incomplete combustion. C surface sites are oxidized by steam with the generation of H_2 and CO_2 that causes activation of biochar surface. Additionally, new porosities are created and smaller pores are enlarged during steam activation (Lima et al., 2010).

5.2.2. Microwave modification

In comparison to the conventional pyrolysis process, biochar modified by microwaves has a higher surface area and more surface functional groups (Wan et al., 2009). Also, the addition of a few target chemicals to biochar activated by microwaves yields superior results (Menendez et al., 2004).

5.2.3. Ball milling

Grinding of biochar into powder during ball milling leads to a reduction in particle size with an increase in specific surface area that further increases the adsorption sites for various ions present in wastewater

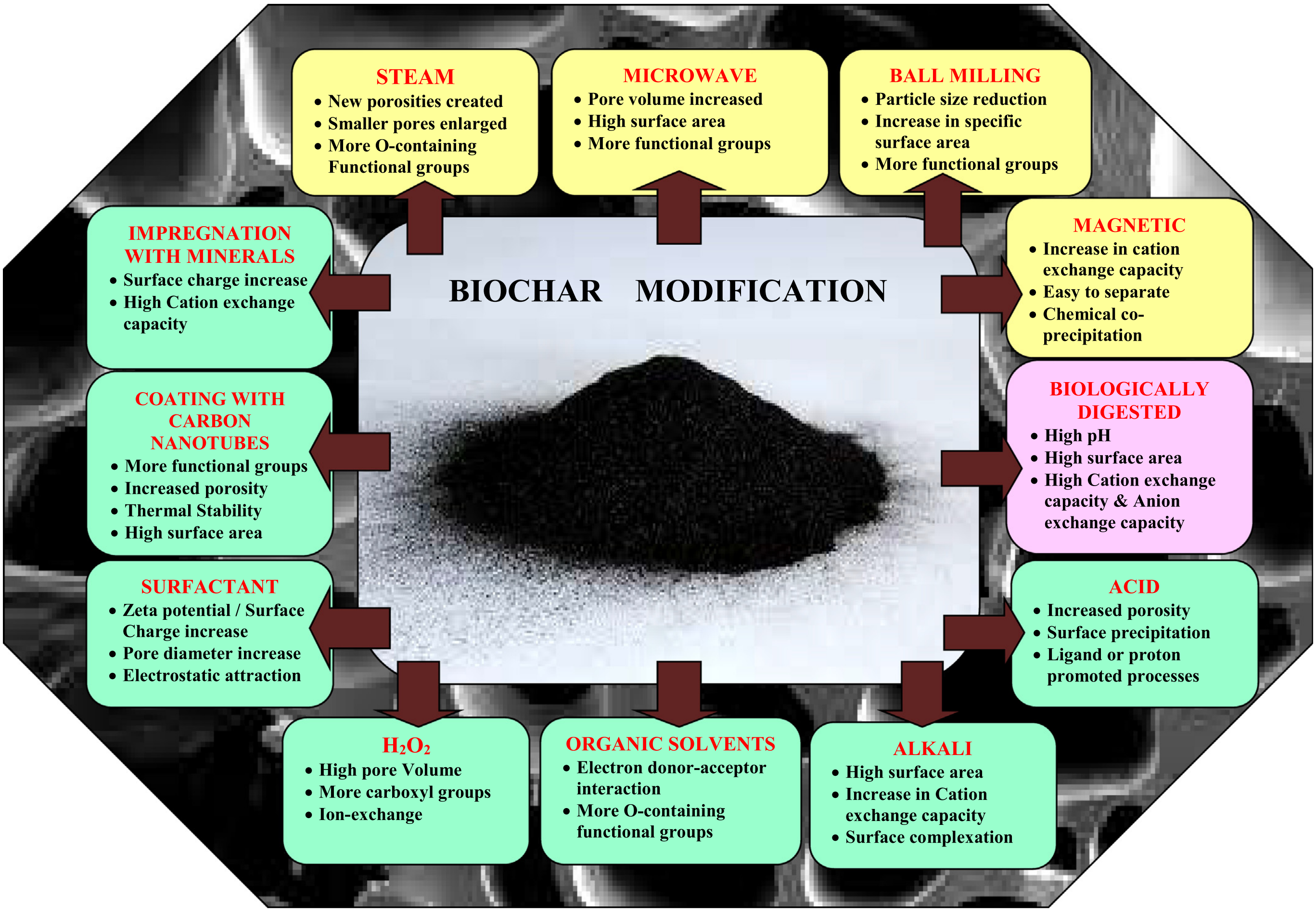

Fig. 5. Different modification methods and their effects on properties of engineered biochars.

(Lyu et al., 2018). Owing to nanoparticle sizes of biochar modified by ball milling, its performance is equivalent to carbon nanotubes. However, due to the easy dispersion and transportation of ball-milled biochar in water, its use in water, as well as soil remediation, is restricted.

5.2.4. Magnetic modification

Biochar activated by magnetic modification (a sort of magnetic material) shows controlled movement under influence of external magnetic fields and thereby, enhanced adsorption and easy to separate properties. Magnetically modified biochars are supplemented with oxides of iron like Fe(O), γ-Fe_2O_3, Fe_3O_4, $CoFe_2O_4$ which leads to strong metal binding (Zhang et al., 2013; Zhou et al., 2014).

For instance, residues from *Oedogonium* spp. (Roberts et al., 2013; Ellison et al., 2014; Roberts et al., 2015e) and *Gracilaria* spp. (Roberts et al., 2015d) left after agar extraction has shown to be efficient in producing Fe-based biosorbent. Another macroalga *Enteromorpha prolifera* was used for the production of magnetic biochar (Chen et al., 2018a). However, there was a reduction in the specific surface area activated algal biochar in comparison to the pristine biochar owing to the loading of iron oxide particles over the surface of biochar that caused blockage of pores. Further, Lalhmunsiama et al. (2017) studied the elimination of Cd(II) and Pb(II) by the magnetic biomaterial which was prepared by impregnating iron oxide nanoparticles with the *Chlorella vulgaris*.

Biochar derived using wasted marine macro-algae (kelp and hijikia) and doped with iron oxide particles (Fe_2O_3, γ-Fe_2O_3, and Fe_3O_4) on its surface, impart magnetism to it (Son et al., 2018). Magnetic biochar, thus developed, have a low surface area, and high removal efficiency for heavy metals in comparison to the conventional pinewood sawdust biochar. Increased efficiency is ascribed to oxygenated functional groups present on magnetic biochar. Though magnetic biochar presents advantages of easy separation, biochar's surface pores become plugged with iron oxide particles causing a reduction in its sorption efficiency. Therefore, to prepare magnetic biochar, the optimum concentration of the iron-loaded solution is resoluted to be 0.025–0.05 mol/L (Son et al., 2018).

5.2.5. CO_2 activation

In this endothermic process, CO_2 acts as an oxidizing agent function between 200 and 900 °C and results in the formation of new pores and widening of existing pores. CO_2 is less reactive and hence used instead of steam to promote steer oxidation reaction and produce the same pore-sized biochar (Anto et al., 2021). However, steam-activated biochar is more active than CO_2-activated biochar because steam is capable of forming a greater number of oxygenated functional groups on biochar (Feng et al., 2016).

5.3. Chemical activation

For producing chemically modified biochar, different chemicals are added during the pyrolysis process (Rajapaksha et al., 2016). Chemically modified biochars have high sorption capacity owing to their increased surface area, surface complexation, surface precipitation, and creation of abundant sorption sites.

5.3.1. Modification by altering the oxidation process and treating biochar with acids and bases

Chemical modification of biochar is done by treating it with acids or bases such as phosphoric acid (H_3PO_4), sulphuric acid (H_2SO_4), nitric acid (HNO_3), and hydrochloric acid (HCl) that modify the porous structure and enhances surface acidities of biochar (Lin et al., 2012). Further, modification of surface functional groups is carried out by oxidation with ozone (O_3), hydrogen peroxide (H_2O_2), ammonium persulfate [$(NH_4)_2S_2O_8$], and potassium permanganate ($KMnO_4$) (Cho et al., 2010; Uchimiya et al., 2011).

Among many, phosphoric acid (H_3PO_4) is an environmental-friendly activating agent that decomposes aliphatic, aromatic, and lignocellulosic compounds (Sun et al., 2011). H_3PO_4 forms polyphosphate and phosphate cross bridges that prevent shrinkage of biochar during the development of porous structures (Fierro et al., 2010; Yang et al., 2011). However, HNO_3 treatment, owing to its erosive nature shows micropore wall degradation, thereby causing a reduction in the surface area of biochar (Stavropoulos et al., 2008). On the contrary, organic acids like oxalic acid undergo ligand- and proton-promoted processes that result in increased sorption capacity of biochar (Vithanage et al., 2015). Acid treatment of biochar is harmful to the environment owing to the disposal of the activation media and also not cost-effective. In comparison, H_2O_2 is a low cost and cleaner agent for modifying and improving the sorption capacity of biochar.

The rise in O content and surface basicity of biochar modified using alkalies like potassium hydroxide (KOH) and sodium hydroxide (NaOH) has been reported (Fan et al., 2010). Treatment with KOH or NaOH was reported to generate activated biochar with a very high surface area (Chia et al., 2015). NaOH has been considered more cost-effective as well as corrosion-resistant for activation of biochar in comparison to KOH (Cazetta et al., 2011).

5.3.2. Carboxylation and amination (modification of functional groups)

Carbonyl, carboxylic, lactonic, and phenolic are oxygenated functional groups that are created over chemically activated biochar surface by using acids like nitric acid (HNO_3), sulphuric acid (H_2SO_4), H_3PO_4, and other compounds like potassium permanganate ($KMnO_4$), hydrogen peroxide (H_2O_2) (Li et al., 2014; Qian et al., 2015). On the contrary, amide, imide, pyrrolic, pyridinic, and lactame (N-containing functionalities) show strong affinities for complexation with metal cations like Cu, Zn, Cd (Shafeeyan et al., 2010). Biochars produced between the temperature range of 250–400 °C have comparatively more C—H and C═C functional groups than the chars produced at high temperatures (Novak et al., 2009).

Functional groups containing nitrogen can be introduced on biochar surfaces by two processes: nitration and reduction; nitration being followed by reduction. It is the surface of biochar where HNO_3 disintegrates into highly active nitronium ions and these ions convert into nitrated products after reacting with aromatic rings. Furthermore, the addition of reducing agents like sodium dithionite ($N_2S_2O_4$) subsequently reduces nitro-groups into amino groups and provides basic properties to the biochar surface (Yang and Jiang, 2014).

5.3.3. Surfactant modifications

By modifying the surface properties of bentonite and zeolite with help of surfactants, more efficient biochars can be produced. Cationic surfactants like cetylpyridinium chloride (CPC), cetyltrimethyl ammonium bromide (CTAB) can be easily captured by negatively charged surface of biochar by processes like electrostatic attraction, and replacement with different cations (Mg^{2+}, Na^+, K^+) present in biochar that finally leads to the formation of "surfactant-biochar" complex (Erdinç et al., 2010). Nonionic surfactants are sorbed by charcoal via physisorption (Santhanalakshmi and Balaji, 1996), however, micellar and monomolecular anionic surfactants are not sorbed on biochar surface due to electrostatic repulsion.

5.3.4. Modifications by treating with organic solvents

In comparison to pristine biochar, biochar modified with methanol has the presence of ester and hydroxyl groups. These functionalities ease the development of electron-donor-acceptor (EDA) interactions between organic contaminants and biochar surfaces (Jing et al., 2014).

5.4. Biochar coating

Biochars coated with metal oxides have enhanced sorption capacity (Wang et al., 2012).

5.4.1. Modifications by coating with oxides of metal

By inserting positively charged metal oxides on the negatively charged high surface area of biochars, biochar-based composites are prepared. Coating biochars with oxides of metals is done by soaking biochar in metal and salt solutions mainly containing nitrates and chlorides, respectively. These modified biochars can remove oxyanions from aqueous solutions proficiently (Beesley et al., 2015).

Biochars can also be modified by impregnating them with minerals (Yao et al., 2014). Biochars impregnated with hydrous aluminium phyllosilicates (clay minerals) have been widely exploited for pollutant removal due to their distinctive surface charge, CEC, and mineralogical structure. Some clay minerals used as low-cost adsorbents are montmorillonite and kaolinite (Rajapaksha et al., 2012).

5.4.1.1. Use of carbon nanotubes (CNTs) coatings for modifications. CNTs are highly efficient in the removal of pollutants owing to their nanostructure and high surface area but their application in wastewater treatment is still limited due to their expensive nature. To overcome this drawback, biochars are used as a porous (micro-and macro-) carrier of CNTs to generate recyclable and efficient sorbents for contaminant removal. On the surface of biochar, coating of functional nanoparticles is carried out to generate a composite material that shows improvement in properties like thermal stability, porosity, surface functionalities, and surface area of biochar (Inyang et al., 2015; Wang et al., 2017).

Although nanoparticles-based-biochar composites have advantages like increased biochar yield and specific surface area, the potential risk on the environment due to biological toxicity of metal oxide nanoparticles (ZnO, TiO_2, CuO, MgO, MnOx, etc.) should also be considered (Tan et al., 2016). Thus, physico-chemical interactions of these biochars with environmental media, their potential eco-toxicity, and economic aspects should be studied before their applications.

5.4.2. Coating with graphene

Graphene has a special two-dimensional structure in addition to certain distinctive properties viz. thermal- and electro-conductivity, mechanical strength, and surface area (Chen et al., 2010). However, like CNTs, difficulty in separation and recovery for reuse explains its restricted use in wastewater treatment. By using a composite of graphene covering particles (that are derived using biochar as graphene carrier), the above-discussed drawbacks can be overcome. Macroalgae are very rich in proteins, thus they can directly form typical nitrogen-doped biochars in situ without any additional modifications (Jung et al., 2016). The sorption of polyaromatic hydrocarbons (PAHs) is supported by graphene structure and facilitated by the presence of N as N enhances π-π electron donor-accepter interaction with benzene rings. Due to lack of lignocellulose, specific surface area, pore structure and pore volume of corresponding biochars are always scarce (Poo et al., 2018; Xiao et al., 2018).

5.5. Other modification methods

Some other modification methods such as low-temperature plasma (Bird et al., 2010; Wu et al., 2012), organic matter grafting (S. Wang et al., 2018), and ozone oxidation (Jimenez-Cordero et al., 2015) have also been studied. Due to their expensiveness and complicated operation, these methods are not applied widely. In the low-temperature plasma method, plasmas are generated by glow, microwave, and corona which then colloid with C═C on biochar surface, and get oxidized to form oxygenated functional groups. Biochars prepared by this method have increased polarity (Yang et al., 2019). In another study, magnetically recoverable biochar supported ternary $g\text{-}C_3N_4/Bi_2O_2CO_3/CoFe_2O_4$ heterojunction was fabricated that showed a high visible photoactivity (Kumar et al., 2018). A high degradation of pesticide paraquat (99.3%) was achieved under visible radiation in 90 min and 92.1% under solar light in 120 min.

A novel concept of e-biochar (i.e., electroactive biochar), to improve electrochemical interactions with microorganisms has emerged in recent times (Schievano et al., 2019). Biochars are also called “geobatteries” because they act as rechargeable reservoirs of bioavailable electrons. e-biochar is perfect to be used as bioelectrode for wider microbial electrochemical technologies (METs) applications in comparison to traditional carbon conductors owing to its wide availability, biocompatibility, and recyclable nature.

6. Application of engineered algal biochar in contaminant remediation

Among different biomaterials, research on macroalgae has drawn interest during recent times for creating carbon nanostructure with high adsorption potential, owing to its high carbon content and reproduction rate along with economic nature. To study the sorption potential of algal biochar, various studies have been carried out recently on different algal species for removal of different pollutants viz. *Porphyra tenera* for Cu(II) (Park et al., 2016); *Spirulina platensis* for Congo red dye (Nautiyal et al., 2016); *Enteromorpha prolifera* for polycyclic aromatic hydrocarbons (PAHs) (Qiao et al., 2017); and *Scenedesmus dimorphus* for Co(II) (Bordoloi et al., 2017). In all the above studies, sorption capacities of biochar ranged between 0.05 and 23.00 mg g^{-1}, showing low values in comparison to the biochar derived from lignocellulosic feedstock.

Therefore, there is an immediate need to search for technologies for the improvement of the adsorption capacity of biochars derived from algae. Table 3 shows different modification methods of algal biochars and their impact on pollutant removal. Biomass of marine macroalgae, particularly, *Porphyra tenera*, *Laminaria japonica*, and *Undaria pinnatifida* show significant prospective for biochar fabrication (Jung et al., 2016). The high adsorption potential of *L. japonica*-based biochar is exploited to produce a modified form of biochar, i.e., granulated biochar ensnared in calcium-alginate beads named *L. japonica*-derived biochar calcium alginate beads (LB-CAB). LB-CAB shows the highest value of adsorption capacity for aqueous phosphate remediation than any other type of biochar (Table 4). The high adsorption potential of LB-CAB is due to its large surface area, and a mature and complex mesopores network.

Seaweed-derived biochar showed high adsorption capacity for phenol with 98.31% removal (Rathinam et al., 2011). *Sargassum* sp. derived biochar modified by lanthanum is also capable of fluoride removal by adsorption process (Y. Yu et al., 2015). Furthermore, *S. platensis* biomass can remove Congo red dye from textile wastewater by 82.6% (Nautiyal et al., 2016). Halide-modified biochar derived from seaweeds can remove elemental mercury (Hg) from flue gas (Liu et al., 2018). Likewise, biochar derived from *Chlorella* sp. is highly efficient in p-nitrophenols removal from wastewater (Zheng et al., 2017).

A modified form of carbonized kelp biochar (AKB) is found quite efficient in the removal of dyes. The modification was done by impregnating AKB with KOH and photocatalytic Bi_2MoO_6/AKB composite (BKBC) nanomaterials (Zhou et al., 2018). The authors reported 61.39% and 94.12% removal of methylene blue (MB) for BKBC and AKB, respectively. When compared with pure Bi_2MoO_6, the MB removal was 13 times and 20 times higher and was ascribed to the large specific surface area of AKB and rich presence of surface functionalities such as —OH and ═C—H.

Innovative Fe-biochar can be created from *Gracilaria* sp. and *Oedogonium* sp. by treating them with a 12.5% *w/v* Fe^{3+} solution, followed by slow pyrolysis. Activated biochar derived from *Oedogonium* sp. shows greater sorption potential for different elements (As, Mo, and Se) in comparison to the *Gracilaria* derived biochar (Johansson et al., 2016). Magnetically modified biochar produced from *Enteromorpha prolifera* is less porous, however, $\gamma\text{-}Fe_2O_3$ encumbered on it helps to remove Cr(VI) effectively (Chen et al., 2018a). After adsorption of Cr(VI) on biochar surface, alterations occur in —OH groups which suggests that the most probable mechanism for Cr(VI) removal is electrostatic interactions.

Table 3

Impact of different modification methodologies on algal biochars and their effect on contaminant remediation.

Modification method	Biochar feedstock	Production temperature	Target sorbate	Effect	Mechanism	Reference
Alkaline modification by 2 M KOH	Anaerobically digested algae-dairy-manure slurry	500 °C	Cu(II)	Alkali activation enhanced the Cu(II) adsorption capacity of biochar which was >3.36 times of pristine biochar.	Total pore volume showed significant increase (~5 times higher) after alkali activation. After modification, alcoholic or phenolic (—OH), aromatic (—CH), carboxylic (C═O), aromatic (C—C), and alkene (═C—H) groups increased on biochar surface, that participated in Cu(II) adsorption	Jin et al. (2016)
Modification with $FeCl_3$ to form Fe biochar	*Gracilaria* waste and *Oedogonium*	400 °C	Mo, As, Se	*Gracilaria* modified Fe biochar showed highest biosorption for Mo (78.5 $mg\ g^{-1}$), followed by As (62.5 $mg\ g^{-1}$) and Se (14.9 $mg\ g^{-1}$). *Oscillatoria* modified Fe biochar showed highest biosorption capacity for As (80.7 $mg\ g^{-1}$,), followed by Mo (67.4 $mg\ g^{-1}$) and Se (36.8 $mg\ g^{-1}$).	Fe-biochar produced at 400 °C tends to have a larger average pore size than Fe-biochar produced at 250 and 700 °C, which plays role in metal sorption	Johansson et al. (2016)
Formation of SiO_2-biochar nanocomposite by using vermiculite treated algal biomass	Algal spp.	500 °C	PO_4^{3-}	SiO_2-biochar nanocomposite showed very high adsorption capacity for PO_4^{3-}	SiO_2 particles on the carbon surface served as sorption sites through electrostatic interactions. The BET surface area, pore diameter, and total pore volume of modified biochar were 42.43 $m^2\ g^{-1}$, 5.17 nm, and 0.055 $cm^3\ g^{-1}$, respectively; while those of pristine biochar were 8.07 $m^2\ g^{-1}$, 11.70 nm, and 0.024 $cm^3\ g^{-1}$. respectively. This increased PO_4^{3-} adsorption process.	Wang et al. (2016)
N-doping	*Ulva prolifera*	200 °C	Bisphenol A	The adsorption capacity for BPA was 33.33 $mg\ g^{-1}$, which was much higher than that of many adsorbents	Biochar had large BET specific surface area and plenty of pores, indicating its high adsorption potential. The FTIR spectra indicated the abundance of basic nitrogen-containing groups	Lu et al. (2017)
Microalgal-biochar immobilized complex	*Chlorella*	–	Cd(II)	The Cd(II) adsorption capacity of modified biochar (217.41 $mg\ g^{-1}$) was higher than that of pristine biochar (95.82 $mg\ g^{-1}$).	Electrostatic adsorption was the mechanism. Negative charges on the surface of biochar boosted the magnetic intensity surrounding the microalgae, which enhanced the surface potential of modified biochar.	Shen et al. (2017)
Magnetic modification with $FeCl_3$	*Enteromorpha prolifera*	600 °C	Cr(VI)	Maximum adsorption capacity of Cr(VI) by the magnetic biochar (91.5 $mg\ g^{-1}$) was far greater than that of pristine biochar.	Change in the —OH groups on the surface after adsorption confirmed that electrostatic interaction was the mechanism for Cr(VI) adsorption	Chen et al. (2018a)
Magnetic modification (doped iron oxide particles)	*Saccharina japonica* (kelp) and *Sargassum fusiforme* (hijikia)	500 °C	Cd^{2+} Cu^{2+} Zn^{2+}	Showed high selectivity for Cu^{2+}, two-fold greater removal (69 $mg\ g^{-1}$ for kelp magnetic biochar and 63.52 $mg\ g^{-1}$ for hijikia magnetic biochar) than Zn^{2+} and Cd^{2+}.	High heavy metal removal performance was due to abundant presence of various oxygen-containing functional groups (—COOH and —OH) on the magnetic biochar	Son et al. (2018)
Algal biochar reinforced trimetallic nanocomposite (AlBc TNC)	Algal spp.	400 °C	malachite green dye	94% of MG dye was remediated using the adsorptional/photocatalytic process.	Modified biochar has high surface area of 107.2 $m^2\ g^{-1}$ with a pore size of 13.23 nm and pore volume of 0.763 $cm^3\ g^{-1}$. Photo-degradation of MG was through production of superoxide anion radicals or hydroxyl radicals.	Sharma et al. (2019)
Composite beads obtained by interaction of algal biomass with PEI, followed by ionotropic gelation and crosslinking processes using $CaCl_2$/glutaraldehyde	*Laminaria digitata*	90 °C	As(V)	Quaternization of algal/PEI beads increased the sorption properties of the composite beads	Anion-exchange of chloride ions with $H_2AsO_4^-$ in acidic conditions.	Hamza et al. (2020)
Magnetic algal carbon supported flower-like	*Ulva prolifera*	180 °C	Bromate (BrO_3^-)	More than 98% of bromate removed within 48 min by the	Chemical reduction by S-nZVI nanoparticles supported on algal	Lu et al. (2020)

Table 3 (*continued*)

Modification method	Biochar feedstock	Production temperature	Target sorbate	Effect	Mechanism	Reference
sulfidated nanoscale zerovalent iron (S-nZVI/AC)				S-nZVI/AC composite	carbon was the main removal process for BrO_3^-. Specific surface area of S-nZVI/AC (56.3 $m^2\ g^{-1}$) was higher than pristine biochar (25.7 $m^2\ g^{-1}$)	
Acid treated biochar	*Spirulina*	350–700 °C	Dyes; rhodamine B, methylene blue, Congo red, and methyl orange	Compared to acid-treated biochar, pristine biochar showed high sorption potential due to high content of inorganic minerals.	Compared to acid-treated biochar, pristine biochar has a high content of Ca^{2+} and Na^+. Due to acid washing various functional groups were removed from modified biochar.	Tan et al. (2020)
Magnetically modified by γ-Fe_2O_3 particles	*Enteromorpha prolifera*	800 °C	Cr(VI)	Magnetic biochar had higher surface polarity, specific surface area, exhibited higher sorption capacity (95.23 $mg\ g^{-1}$) compared with pristine biochar.	Modified biochar has more oxygen-containing functional groups. Main mechanisms were chemisorption and monolayer electrostatic adsorption	Y. Wang et al. (2020)
$Fe_3O_4^-$ modified biochar	*Microcystis aeruginosa*	200 °C	U(VI)	The maximum sorption capacity of pristine biochar was higher than that of Fe_3O_4/MB.	U(VI) sorption on both pristine and modified biochar was ascribed to surface complexation between U(VI) and oxygen-containing functional groups. Fe_3O_4 particles on surface of modified biochar didn't provide extra active sites for U (VI) sorption	B. Wang et al. (2020)
Magnetic *U. prolifera* biochar/sulfidated Fe^0 composite (S-Fe^0/BC)	*Ulva prolifera*	180 °C	Tetrabromo-bisphenol A	Removal efficiency by S-Fe^0/BC composite within 24 h was 88.2%, higher than that in pristine biochar (55.3%)	The removal process of TBBPA by modified biochar was chemical adsorption by S-Fe^0/BC composite, reduction debromination by S-Fe^0 and enhanced electron transfer.	Zhang et al. (2020)

N-doped algal biochar prepared from *U. prolifera* is featured with a high specific surface area (25.43 $m^2\ g^{-1}$) and a huge number of pores in comparison to other algal biochars (<5 $m^2\ g^{-1}$) (Bird et al., 2011; Lu et al., 2017). FTIR spectral studies reported that functional groups containing nitrogen are present on the surface of activated biochar. As high temperature increases the adsorption of Bisphenol-A on the surface of biochar, adsorption is suggested to be an endothermic process.

Modification of biochar prepared from anaerobically digested algae-dairy-manure slurry by adding alkali (2 M potassium hydroxide) reports an increase in Cu(II) sorption capacity of activated biochar by 3.36 times in comparison to pristine biochars (Jin et al., 2016). The enhanced sorption capacity of activated biochar is due to its increased surface area, changed porous texture, and surface functionalities. On the contrary, KOH activated red macroalgae, *Porphyra tenera*, despite high surface area and greater pore volume reduces only a little of copper (Park et al., 2016). A rise in solution pH during adsorption accelerates the hydrolysis of Cu(II) to form $Cu(OH)^+$ and $Cu(OH)_2$, which further leads to easy adsorption and precipitation of Cu(II) (Tong et al., 2011).

On the evaluation of the pH effect, Kim et al. (2016) reported maximum Cu(II) sorption capacity of activated biochar derived from *Enteromorpha compressa* at pH ~ 5.5. Following the speciation diagram, at pH below 5.5, the dominance of Cu^{2+} prevails, however, with an increase in pH over 6, Cu^{2+} is converted into $Cu(OH)^+$ and finally precipitates as $Cu(OH)_2$.

Structure and morphology analysis of the SiO_2-biochar nanocomposites derived from vermiculite treated algal biomass sample reveals the uniform distribution of nanosized SiO_2 particles on biochar surface (Wang et al., 2016). These SiO_2 particles serve as sorption sites through electrostatic interactions thus showing greater removal of phosphate from solution in comparison to pristine biochar. Oxygenated functional groups enhance the removal of Cu^{2+} by algal magnetic biochar (Cho et al., 2013). Biochar prepared from *Saccharina japonica* and *Sargassum fusiforme* contains a large number of oxygenated functional groups and has a high pH value, therefore they can efficiently remove Cu, Cd, and Zn by adsorption from an aqueous solution (Poo et al., 2018). Chen et al. (2018b) reported a the highest dye removal capacity at 800 °C using algal biochar. At neutral pH, cationic malachite green and crystal violet dye were found to be adsorbed more than Congo red anion owing to electrostatic attractions. At low pH, p-p donor-acceptor interaction remained the adsorption mechanism, and at high pH, negative charge-assisted H-bond was found to be the adsorption mechanism. Biochar prepared from *Chlorella* sp. has a higher adsorption capacity for p-nitrophenol due to the presence of abundant oxygen-containing functional groups (Zheng et al., 2017; Chen et al., 2020).

Furthermore, Hung et al. (2020) used biochar synthesized from red algae-*Agardhiella subulata* and performed remediation of 4-Nonylphenol (4-NP). They found that sufficient catalytic sites (having Ca^{2+} ions) provided by the mineral phase of CaO, facilitated the electron transfer reaction at the RAB surface towards catalytic 4-NP decomposition. Further, FTIR analyses of RAB revealed the presence of different oxygen-containing functional groups (OFGs) viz. O—H, C—O—C, C—O bonds, and —COOH, —COO— groups. OFGs were found as active catalytic sites and electron acceptors for 4-NP oxidation. Also, OFGs presence on the RAB surface enhanced the generation of HO according to the following reactions, which further enhanced 4-NP degradation (Hung et al., 2020).

$$RAB{-}OH + H_2O_2 \rightarrow RAB{-}O^{\cdot} + HO^{\cdot} + H_2O \tag{1}$$

$$RAB{-}OOH + H_2O_2 \rightarrow RAB{-}OO^{\cdot} + HO^{\cdot} + H_2O \tag{2}$$

$$RAB{-}OOH + H_2O_2 \rightarrow RA{-}OH + H_2O + O_2 \tag{3}$$

Biochars have also been manufactured from C-phycocyanin extracted (C-CP) *Spirulina* residue (SDBC) via thermal pyrolysis (Ho et al., 2019). Concurrently, N-doping was attained from the protein in

Table 4
Maximum biosorption capacity of algal biochars/engineered algal biochars for diverse contaminants.

Algal biochar	Contaminant	Biosorption capacity	Reference
Undaria pinnatifida	Cu^{2+}	125.85 mg g^{-1}	Cho et al. (2013)
Anaerobically digested algae-dairy-manure slurry	Cu^{2+}	50.71 mg g^{-1}	Jin et al. (2016)
Gracilaria modified biochar (GMB) *Oedogonium* modified biochar (OMB)	Mo As Se	**GMB** Mo: 78.5 mg g^{-1} As: 62.5 mg g^{-1} Se: 14.9 mg g^{-1} **OMB** Mo: 67.4 mg g^{-1} As: 80.7 mg g^{-1} Se: 36.8 mg g^{-1}	Johansson et al. (2016)
Laminaria japonica-derived biochar calcium alginate beads	PO_4^{3-}	157.7 mg g^{-1}	Jung et al. (2016)
Enteromorpha compressa	Cu^{2+}	137 mg g^{-1}	Kim et al. (2016)
Spirulina platensis	Congo red dye	51.28 mg g^{-1}	Nautiyal et al. (2016)
Ulva prolifera	Bisphenol A	33.33 mg g^{-1}	Lu et al. (2017)
Chlorella	Cd	169.92 mg g^{-1}	Shen et al. (2017)
Chlorella	p-Nitrophenols	204.80 mg g^{-1}	Zheng et al. (2017)
Magnetically modified *Enteromorpha prolifera*	Cr(VI)	88.17 mg g^{-1}	Chen et al. (2018a)
Ulothrix zonata	Malachite green, Congo red, crystal violet	5306.20, 1222.50, 345.20 mg g^{-1}	Chen et al. (2018b)
Saccharina japonica *Sargassum fusiforme*	Cu Cd Zn	98.60, 60.70, 84.30 mg g^{-1} 94.10, 37.20, 43.00 mg g^{-1}	Poo et al. (2018)
Marine macroalgae Kelp Hijikia	Cd^{2+} Cu^{2+} Zn^{2+}	**Kelp** Cd^{2+}: 23.16 mg g^{-1} Cu^{2+}:55.86 mg g^{-1} Zn^{2}: 22.22 mg g^{-1} **Hijikia** Cd^{2+}: 19.40 mg g^{-1} Cu^{2+}: 47.75 mg g^{-1} Zn^{2}: 19.13 mg g^{-1}	Son et al. (2018)
Vermiculite-modified algal biochar	PO_4^{3-}	159.4 mg g^{-1}	Wang et al. (2016)
Carbonized kelp biochar modified by KOH impregnation	Methylene blue	324.1 mg g^{-1}	Zhou et al. (2018)
Caulerpa scalpelliformis	Remazol brilliant blue R, Remazol brilliant orange 3 R, Remazol brilliant viole 5 R, Remazol black B	0.178, 0.231, 0.217, 0.228 mmol g^{-1}	Gokulan et al. (2019)
Cladophora glomerata	Cr(III)	87.1 mg g^{-1}	Michalak et al. (2019)
Spirulina sp.	Tetracycline	132.8 mg g^{-1}	Choi et al. (2020)
High-salinity *Spirulina* residue	Hg(II)	12.7 mg g^{-1}	Ge et al. (2020)
High-salinity *Spirulina* residue	rhodamine B methylene blue Congo red methyl orange	421.93 mg g^{-1} 370.24 mg g^{-1} 287.89 mg g^{-1} 177.32 mg g^{-1}	Tan et al. (2020)
Enteromorpha prolifera	Cr(VI)	95.23 mg g^{-1}	Y. Wang et al. (2020)
Chlorella	Methylene blue Congo red	113.00 mg g^{-1} 164.35 mg g^{-1}	Yu et al. (2020)
Magnetic *Ulva prolifera* biochar/sulfidated Fe0 composite	Tetrabromobisphenol A (TBBPA)	27.4 mg g^{-1},	Zhang et al. (2020)
Eucheuma spinosum	Red 120 dye	331.97 mg g^{-1}	Gurav et al. (2021)

the algae for gaining a high-performance carbon catalyst for *peroxydisulfate* (PDS) activation. The SDBC yielded large specific surface areas, nitrogen loading, and good conductivity, with outstanding oxidation efficiencies to widespread aqueous microcontaminants.

Three-dimensional graphene-like biochar derived from *Enteromorpha* (EGB) was manufactured as a persulfate (PS) activator for sulfamethoxazole (SMX) degradation (Qi et al., 2020). The graphitic N in the EGB samples not only endowed the superior binding energy towards SMX adsorption but also promoted the PS binding with the EGB, which was crucial to the catalytic degradation of SMX in the EGB/PS system. In another study, enhanced macroalgal biochars were fabricated by co-carbonization of macroalgae (*Enteromorpha prolifera* and *Ulva lactuca*), ferric chloride, and zinc chloride (PGNBC). These hydrophobic biochars possess large specific surface areas (up to 399 m^2 g^{-1}), high nitrogen doping (up to 6.14%), and a partly graphitized structure (Cheng et al., 2020). This study described the sorption process as; PAHs first sorb onto PGNBCs surface by pore filling, π–π stacking and partition effect, and then transferred into interspaces of PGNBC through same mechanisms.

H. Wang et al. (2020) synthesized an innovative biochar composite infused with α-Fe_2O_3 in Fe(III)-ABC-20 (a hierarchical porous structure) from Taihu blue algae through KOH combined pyrolysis. This novel biochar had a high specific surface area of 1657.8 m^2 g^{-1} and abundant O-containing functional groups on its surface. This biochar composite also displayed 98.87% removal of chelated nickel from electroplating wastewater.

The algal biochar reinforced trimetallic nanocomposite (AlBc TNC) was fabricated using the facile greener microwave technique (Sharma et al., 2019). AlBcTNC was considered as a suitable adsorbent/photocatalyst designed for the exclusion of malachite green (MG). The study showed that the fabricated AlBcTNC has good adsorptional/photocatalytic potential towards the remediation of MG. 94% of MG dye was removed by the adsorptional/photocatalytic process.

In a study conducted by Ge et al. (2020) for Hg(II) removal, calcium and chloride minerals were observed to be formed in high-salinity *Spirulina* residue (HSR) derived biochar (HSRBC). Based on dual-mode isotherm, surface sorption and precipitation of Hg(II) accounted for 75–88% and 12–25% uptake, respectively. Also, C—O, C═O, and C═C groups induced monodentate/bidentate complexation and reduction, while Cl^- triggered Hg_2Cl_2 precipitation.

7. Bioelectrochemical systems using engineered and/or algal biochar

In some studies, it has been reported that biochar shows immense compatibility in the promotion of interspecies electron transfer as well as the formation of colonies by functional microorganisms (Luo et al., 2015). On the same line, algal bloom derived biochar can be used as an anode for extracellular electron uptake in Bioelectrochemical systems (BESs) and where *Shewanella oneidensis* act as a model electricity-producing strain (Y.S. Wang et al., 2018). This biochar-derived anode efficiently exploits both direct as well as mediated electron transfer pathways (ETPs). Furthermore, biochar-derived anode shows high adsorption of the redox mediator and a more powerful electrochemical response in comparison to graphite plate electrodes.

Two different mechanisms are speculated for higher biocurrent production with biochar electrodes derived from an algal bloom. Firstly, bacterial cells that attach onto the electrode surface under the facilitation of algal biochar, contribute towards the direct transfer of electrons between c-type cytochromes through redox reactions. Secondly, algal biochar shows tremendous sorption capacity and electrochemical response for redox mediator that in turn lead to indirect transfer of electrons between electrodes and riboflavin during current generation (doesn't matter whether following direct or indirect electron transfer pathways) in comparison to graphite plate electrode (Y.S. Wang et al., 2018).

A novel and innovative class of biochars i.e., *e*-biochar having tailored conductivity and electron transfer properties are suggested for Microbial electrochemical technologies (METs) application, owing to its wide availability, biocompatibility, and complete recyclability at end-of-life to be used as a soil amendment. *e*-biochar is also defined as an environmentally-sustainable electron acceptor or donor in biogeochemical oxidation-reduction reactions (Yuan et al., 2017). However, long-term biochar remediation could decrease the functional microbial community species. In such cases, the wasted biochar electrodes can be used for soil-based application for possible improvement in the quality of the soil. The direct interspecies electron transfer (DIET) also enables microbial communities to gain energy from reactions that no microbe can catalyze, a mechanism for substituting electrons during syntrophic metabolism. Additionally, the anode biofilms will form electrically conductive aggregates which can further enhance the bioelectrochemical response of the *e*-biochar based system (Ramírez-Vargas et al., 2018).

The conductivity of *e*-biochar depends upon its structural order, like, if the range of crystalline order is longer, the π-electrons are more delocalized leading to high electrical conductivity. Similarly, electron-donating O—, N— and metals functionalities and high aromatic content of the biomass increases the conductivity of *e*-biochars. Conductivity is also increased by high temperatures (>600 °C), slow rates of heating, and longer treatments owing to improvement of structural order (Berenguer et al., 2016). Biochar can stimulate electron transfer more effectively than highly conductive carbon materials viz. graphite and coke and thus show increased removal of pollutants from polluted water in electroactive biofilters (Prado et al., 2019).

To date, four different cell-surface redox proteins are recognized that are accountable for electron transfer across cell-surface of electroactive organisms. Out of four, cell-surface exposed cytochromes are prime cellular components that interact with solid conductors. Exchange of electrons with solid electron donors or acceptors outside the cell is allowed with redox proteins that form conductive ET chains (Costa et al., 2018). Also, various electroactive microorganisms utilize cellular structures, like nanowires or pili to improve ET (Gorby et al., 2006).

Bioelectrodes can be fabricated by carbonization of lignocellulosic biomass; their original 3-D shape is to be preserved during the manufacturing process. Wild mushrooms, marine loofah sponges, corn cobs are suitable for bioanode formation (Yuan et al., 2013; Li et al., 2014). Air-breathing biocathodes can be derived from giant sugarcane stems that act as microporous air-water separators; their original shape is to be maintained.

Electroconductive granules can act as planktonic electrodes in a bioreactor. Electroconductive granules are fluidized in bioreactor and they support microbial electroactivity there (Tejedor-Sanz et al., 2017). Electrons are accumulated on the material from where they are discharged to a collector site periodically by contact. Such a design in which electroactive material is used and is conceptualized on constructed wetland is applied to the large-scale application of microbial electrochemical technologies (MET). This concept is called 'METland' in which electroconductive material replaces the classical bed biofilter composed of inert materials (Aguirre-Sierra et al., 2016).

Magnetic biochar (MBC) having olive-shaped pores, and functional biochar (FBC) having a three-dimensional pore network can be derived from *Cladophora glomerata* through activation by $FeCl_3$ and KOH and these biochars act as electrodes in supercapacitors. On treating FBC with HNO_3 and H_2SO_4, Fe composite biochar (FCBC) is obtained that serve as electrodes in supercapacitors and shows significant electrochemical behaviors, demonstrating excellent cycle stability and high specific capacitance. Furthermore, by using FBC as anode and iron oxide/carbon composites as a cathode in 3 M KCl electrolytes, an asymmetrical supercapacitor having elevated power and energy densities can also be fabricated (Pourhosseini et al., 2018).

8. Conclusion and future challenges

An escalating curiosity in valuable biochar applications has created multidisciplinary areas for scientific research and engineering. Engineered biochar can be successfully applied in multiple areas such as carbon sequestration, improvement of soil fertility, remediation of water/soil environment, and storage of energy. Owing to its large surface area and special structure, biochar has been efficiently used as a sorbent for removing different contaminants, organic as well as inorganic.

Costs for algal biochar production and its applications in removing pollutants, being a sorbent depend upon various factors. These factors comprise of type and availability of the feedstock; raw material preparation; pyrolysis conditions and regeneration of biochar after its use (Alhashimi and Aktas, 2017). Thus, a major challenge for future optimisation of biochar use is, reduction of the number of chemicals used for activating biochar means optimising biochar: modifying agent ratio thereby minimizing production costs. Besides, strong oxidants like acids, and alkalis used for modification during the production of engineered biochars, impose a risk of secondary pollution to the environment. As a solution, organic acids like tartaric acid, acetic acid, and citric acid can be used as modifiers in a cleaner and greater production of engineered biochars (L. Sun et al., 2015). Therefore, in near future, the development of economic and environment-friendly chemical reagents for algal biochar modification needs further research in relevance.

The impacts of engineered biochar on the chemical properties of soil have been still studied but its effects on soil microorganisms have received very low attention (Lehmann et al., 2011). Also, the application of biochar as a soil conditioner changes the native microbial population of soil. Engineered biochar also consist of clay minerals, nanomaterials, and graphenes that kill soil microbiota and causes toxicity to ecosystems. Certain compounds in biochar are known as microbial inhibitors, viz. benzene, methoxy phenols and phenols, carboxylic acids, ketones, furans, and PAHs (Spokas et al., 2011; Lyu et al., 2016; Ghidotti et al., 2017; Zhu et al., 2017). PFRs (including semiquinones, phenoxyls, cyclopentadienyls, and phenols) generated during pyrolysis, also induce toxicity to microorganisms (Truong et al., 2010). Thus, further evaluation of risk management of engineered algal biochar composites is required before its large-scale environmental applications. *e*-biochar can realize the promises of MET applications more interestingly. To attain this objective, all the existing information on biochar such as its abiotic electrochemistry, surface material chemistry, and nanotechnological information should be strictly in coherence with concepts of bioelectrochemistry, molecular studies on electron transfer, and biofilm ecology. In recent times, vast research has been carried out on engineered biochars, still, these explorations are restricted in laboratories and field theoretical stage. Only a few studies are available on the significant and extensive applications of engineered algal biochars. Fabrication of engineered biochars at an industrial-scale and processes of their specific applications are still in their infancy and hence, need more engineering support and research in future times.

For the practical application of algal biochar, its production cost is a key aspect that hampers its field application (Li et al., 2018). Thus, novel investigations should search for compromises between the biochar feedstock, methods used for modifications, and sorption capacities that reduce costs and enhances its technical applicability. Algal biomass obtained from aquaculture, eutrophied natural waterways, marine resources can be employed as a feedstock for low-cost biochar fabrication. The algal biochar thus produced could provide a major stream for revenue generation shortly through carbon sequestration, energy generation, use as biosorbent, and soil amendment (Bird et al., 2012).

To understand the physicochemical properties of algal biochar, its characterization is imperative, as it will help determine its prospects. For instance, in comparison to biochar generated at high temperatures (>400 °C), one that generates at a temperature between 300 and 400 °C have high toxicities for PAHs, polychlorinated dioxins, and furans (Lyu et al., 2016). The diversified VOC species adsorbed on biochar can be the key reason responsible for many responses of soil microorganisms to biochar. When present in optimum concentrations in fresh biochar, VOCs serve as a carbon source and support the survival of some microorganisms (*Bacillus mucilaginosus*) (D. Sun et al., 2015), but when the concentration exceeds the optimum limit, they can bring potential toxicity to microorganisms (not species-specific) (Ennis et al., 2012). Thus, the changes in the structure of the microbial community triggered by biochar require additional study to assess the environmental risks and benefits of biochar application.

Future research work will primarily deal with optimization of feedstock type, pyrolysis temperature, type of modification that will furnish a versatile group of engineered algal biochars suitable for remediating an array of contaminants under diverse conditions. Furthermore, microwave-assisted technology is also a potential approach in the production of algal biochar that deserves more consideration in near future.

While considering algal feedstock used for the production of biochar, microalgae seem to be comparatively more potential candidate than macroalgae, given their ease of cultivation and harvesting, and rapid growth. Thus, extensive research on various aspects of microalgal biochar comprising production and modification procedures along with microalgal manipulations using uni- and multi-omics techniques to obtain structurally improved bio-engineered algal biochars with simultaneous generation of value-added products, is additionally recommended owing to the scarcity of data on these aspects and to make this technology commercially more attractive (Mishra et al., 2019). Further progression in the field of engineered algal biochar will contribute towards the concept of sustainability of the environment in near future.

Declaration of competing interest

The authors declare that they have no known competing financial interests or personal relationships that could have appeared to influence the work reported in this paper.

References

Abbasi, T., Abbasi, S.A., 2010. Biomass energy and the environmental impacts associated with it's product and utilization. Renew. Sust. Energ. Rev. 14 (3), 919–937.

Abel, S., Peters, A., Trinks, S., Schonsky, H., Facklam, M., Wessolek, G., 2013. Impact of biochar and hydrochar addition on water retention and water repellency of sandy soil. Geoderma 202–203, 183–191.

Aguirre-Sierra, A., Bacchetti-De Gregoris, T., Berná, A., Salas, J.J., Aragón, C., Esteve-Núñez, A., 2016. Microbial electrochemical systems outperform fixed-bed biofilters in cleaning up urban wastewater. Environ. Sci. Water Res. Technol. 2 (6), 984–993.

Ahmad, M., Lee, S.S., Dou, X., Mohan, D., Sung, J.-K., Yang, J.E., Ok, Y.S., 2012. Effects of pyrolysis temperature on soybean stover-and peanut shell-derived biochar properties and TCE adsorption in water. Bioresour. Technol. 118, 536–544.

Ahmad, M., Rajapaksha, A.U., Lim, J.E., Zhang, M., Bolan, N., Mohan, D., Vithanage, M., Lee, S.S., Ok, Y.S., 2014. Biochar as a sorbent for contaminant management in soil and water: a review. Chemosphere 99, 19–33.

Akhtar, A., Jirícek, I., Ivanova, T., Mehrabadi, A., Krepl, V., 2019. Carbon conversion and stabilisation of date palm and high rate algal pond (microalgae) biomass through slow pyrolysis. Int. J. Energy Res. 43 (9), 4403–4416.

Alhashimi, H.A., Aktas, C.B., 2017. Life cycle environmental and economic performance of biochar compared with activated carbon: a meta-analysis. Resour. Conserv. Recycl. 118, 13–26.

Amin, M., Chetpattananondh, P., Khan, M.N., 2020. Ultrasound assisted adsorption of reactive dye-145 by biochars from marine *Chlorella* sp. extracted solid waste pyrolyzed at various temperatures. J. Environ. Chem. Eng. 8, 104403.

Andrade, L., Batista, F., Lira, T., Barrozo, M., Vieira, L., 2018. Characterization and product formation during the catalytic and non-catalytic pyrolysis of the green microalgae *Chlamydomonas reinhardtii*. Renew. Energy 119, 731–740.

Angın, D., 2013. Effect of pyrolysis temperature and heating rate on biochar obtained from pyrolysis of safflower seed press cake. Bioresour. Technol. 128, 593–597.

Anto, S., Sudhakar, M.P., Ahamed, T.S., Samuel, M.S., Mathimani, T., Brindhadevi, K., Pugazhendhi, A., 2021. Activation strategies for biochar to use as an efficient catalyst in various applications. Fuel 285, 119205.

Astals, S., Musenze, R.S., Bai, X., Tannock, S., Tait, S., Pratt, S., Jensen, P.D., 2015. Anaerobic co-digestion of pig manure and algae: impact of intracellular algal products recovery on co-digestion performance. Bioresour. Technol. 181, 97–104.

Azizi, K., Moraveji, M.K., Najafabadi, H.A., 2018. A review on bio-fuel production from microalgal biomass by using pyrolysis method. Renew. Sust. Energ. Rev. 82, 3046–3059.

Bach, Q.-V., Chen, W.-H., Sheen, H.-K., Chang, J.-S., 2017a. Gasification kinetics of raw and wet-torrefied microalgae *Chlorella vulgaris* ESP-31 in carbon dioxide. Bioresour. Technol. 1393–1399.

Bach, Q.-V., Chen, W.-H., Lin, S.-C., Sheen, H.-K., Chang, J.-S., 2017b. Wet torrefaction of microalga *Chlorella vulgaris* ESP-31 with microwave-assisted heating. Energy Convers. Manag. 141, 163–170.

Beesley, L., Moreno-Jimenez, E., Gomez-Eyles, J.L., 2010. Effects of biochar and green waste compost amendments on mobility, bioavailability and toxicity of inorganic and organic contaminants in a multi-element polluted soil. Environ. Pollut. 158, 2282–2287.

Beesley, L., Moreno-Jim_enez, E., Gomez-Eyles, J.L., Harris, E., Robinson, B., Sizmur, T., 2011. A review of biochars' potential role in the remediation, revegetation and restoration of contaminated soils. Environ. Pollut. 159, 3269–3282.

Beesley, L., Moreno-Jimenez, E., Fellet, G., Carrijo, L., Sizmur, T., 2015. Biochar and heavy metals. In: Lehmann, J., Joseph, S. (Eds.), Biochar for Environmental Management: Science and Technology. Routledge, Abingdon, UK.

Berenguer, R., García-Mateos, F.J., Ruiz-Rosas, R., Cazorla-Amorós, D., Morallón, E., Rodríguez-Mirasol, J., Cordero, T., 2016. Biomass-derived binderless fibrous carbon electrodes for ultrafast energy storage. Green Chem. 18 (6), 1506–1515.

Bird, M.I., Charville-Mort, P.D., Ascough, P.L., Wood, R., Higham, T., Apperley, D., 2010. Assessment of oxygen plasma ashing as a pre-treatment for radiocarbon dating. Quat. Geochronol. 2010 (5), 435–442.

Bird, M.I., Wurster, C.M., de Paula Silva, P.H., Bass, A.M., de Nys, R., 2011. Algal biochar production and properties. Bioresour. Technol. 102, 1886–1891.

Bird, M.I., Wurster, C.M., De Paula Silva, P.H., Paul, N., de Nys, R., 2012. Algal biochar: effects and applications. GCB Bioenergy 4, 61–69.

Biswas, B., Kumar, A., Bisht, Y., Singh, R., Kumar, J., Bhaskar, T., 2017. Effects of temperature and solvent on hydrothermal liquefaction of *Sargassum tenerrimum* algae. Bioresour. Technol. 344–350.

Bordoloi, N., Narzari, R., Sut, D., Saikia, R., Chutia, R.S., Kataki, R., 2016. Characterization of bio-oil and its sub-fractions from pyrolysis of *Scenedesmus dimorphus*. Renew. Energy 98, 245–253.

Bordoloi, N., Goswami, R., Kumar, M., Kataki, R., 2017. Biosorption of Co (II) from aqueous solution using algal biochar: kinetics and isotherm studies. Bioresour. Technol. 244, 1465–1469.

Borges, F.C., Xie, Q., Min, M., Muniz, L.A.R., Farenzena, M., Trierweiler, J.O., Chen, P., Ruan, R., 2014. Fast microwave-assisted pyrolysis of microalgae using microwave absorbent and HZSM-5 catalyst. Bioresour. Technol. 166, 518–526.

Bryant, H.L., Gogichaishvili, I., Anderson, D., Richardson, J.W., Sawyer, J., Wickersham, T., Drewery, M.L., 2012. The value of post-extracted algae residue. Algal Res. 1 (2), 185–193.

Canabarro, N., Soares, J.F., Anchieta, C.G., Kelling, C.S., Mazutti, M.A., 2013. Thermochemical processes for biofuels production from biomass. Sustain. Chem. Process. 1 (1), 22.

Cao, X., Harris, W., 2010. Properties of dairy-manure-derived biochar pertinent to its potential use in remediation. Bioresour. Technol. 101, 5222–5228.

Cao, B., Yuan, J., Jiang, D., Wang, S., Barati, B., Hu, Yamin, Chuan, Y., Gong, X., Wang, Q., 2021. Seaweed-derived biochar with multiple active sites as a heterogeneous catalyst for converting macroalgae into acid-free bio oil containing abundant ester and sugar substances. Fuel 285, 119164.

Casoni, A.I., Zunino, J., Piccolo, M.C., Volpe, M.A., 2016. Valorization of *Rhizoclonium* sp. algae via pyrolysis and catalytic pyrolysis. Bioresour. Technol. 216, 302–307.

Cazetta, A.L., Vargas, A.M.M., Nogami, E.M., Kunita, M.H., Guilherme, M.R., Martins, A.C., Silva, T.L., Moraes, J.C.G., Almeida, V.C., 2011. NaOH-activated carbon of high surface area produced from coconut shell: kinetics and equilibrium studies from the methylene blue adsorption. Chem. Eng. J. 174, 117–125.

Cha, J.S., Park, S.H., Jung, S.-C., Ryu, C., Jeon, J.-K., Shin, M.-C., Park, Y.-K., 2016. Production and utilization of biochar: a review. J. Ind. Eng. Chem. 40, 1–15.

Chaiwong, K., Kiatsiriroat, T., Vorayos, N., Thararax, C., 2012. Biochar production from freshwater algae by slow pyrolysis. J. Sci. Technol. 6, 186–195.

Chaiwong, T., Kiatsiriroat, N., Vorayos, C., Thararax, K., 2013. Study of bio-oil and bio-char production from algae by slow pyrolysis. Biomass Bioenergy 56, 600–606.

Chen, D., Tang, L., Li, J., 2010. Graphene-based materials in electrochemistry. Chem. Soc. Rev. 39, 3157–3180.

Chen, M., Kang, X., Wumaier, T., Dou, J., Gao, B., Han, Y., Xu, G., Liu, Z., Zhang, L., 2013. Preparation of activated carbon from cotton stalk and its application in supercapacitor. J. Solid State Electr. 17, 1005–1012.

Chen, W.-H., Huang, M.-Y., Chang, J.-S., Chen, C.-Y., 2014a. Thermal decomposition dynamics and severity of microalgae residues in torrefaction. Bioresour. Technol. 169, 258–264.

Chen, W.-H., Wu, Z.-Y., Chang, J.-S., 2014b. Isothermal and non-isothermal torrefaction characteristics and kinetics of microalga *Scenedesmus obliquus* CNW-N. Bioresour. Technol. 155, 245–251.

Chen, W.-H., Peng, J., Bi, X.T., 2015a. A state-of-the-art review of biomass torrefaction, densification and applications. Renew. Sust. Energ. Rev. 44, 847–866.

Chen, W.-H., Lin, B.-J., Huang, M.-Y., Chang, J.-S., 2015b. Thermochemical conversion of microalgal biomass into biofuels: a review. Bioresour. Technol. 184, 314–327.

Chen, W.-H., Huang, M.-Y., Chang, J.-S., Chen, C.-Y., 2015c. Torrefaction operation and optimization of microalga residue for energy densification and utilization. Appl. Energy 154, 622–630.

Chen, Y.-C., Chen, W.-H., Lin, B.-J., Chang, J.-S., Ong, H.C., 2016. Impact of torrefaction on the composition, structure and reactivity of a microalga residue. Appl. Energy 181, 110–119.

Chen, W., Yang, H., Chen, Y., Xia, M., Chen, X., Chen, H., 2017. Transformation of nitrogen and evolution of N-containing species during algae pyrolysis. Environ. Sci. Technol. 51, 6570–6579.

Chen, Y.D., Wang, B., Xin, J., Sun, P., Wu, D., 2018a. Adsorption behavior and mechanism of Cr(VI) by modified biochar derived from *Enteromorpha prolifera*. Ecotox. Environ. Safe. 164, 440–447.

Chen, Y.D., Lin, Y.C., Ho, S.H., Zhou, Y., Ren, N., 2018b. Highly efficient adsorption of dyes by biochar derived from pigments-extracted macroalgae pyrolyzed at different temperature. Bioresour. Technol. 259, 104–110.

Chen, C., Ma, T., Shang, Y., Gao, B., Jin, B., Dan, H., Li, Q., Yue, Q., Li, Y., Wang, Y., Xu, X., 2019. In-situ pyrolysis of *Enteromorpha* as carbocatalyst for catalytic removal of organic contaminants: considering the intrinsic N/Fe in *Enteromorpha* and non-radical reaction. Appl. Catal. B Environ. 250, 382–395.

Chen, L., Yu, Z., Xu, H., Wan, K., Liao, Y., Ma, X., 2019. Microwave-assisted co-pyrolysis of *Chlorella vulgaris* and wood sawdust using different additives. Bioresour. Technol. 273, 34–39.

Chen, Y.D., Liu, F., Ren, N.Q., Ho, S.H., 2020. Revolutions in algal biochar for different applications: state-of-the-art techniques and future scenarios. Chin. Chem. Lett. 31, 2591–2602.

Cheng, H., Ji, R., Bian, Y., Jiang, X., Yang, S., 2020. From macroalgae to porous graphitized nitrogen-doped biochars – using aquatic biota to treat polycyclic aromatic hydrocarbons-contaminated water. Bioresour. Technol. 303, 122947.

Chia, C.H., Downie, A., Munroe, P., 2015. Characteristics of biochar: physical and structural properties. Biochar for Environmental Management: Science, Technology and Implementation, p. 89.

Cho, H.-H., Wepasnick, K., Smith, B.A., Bangash, F.K., Fairbrother, D.H., Ball, W.P., 2010. Sorption of aqueous Zn[II] and Cd[II] by multiwall carbon nanotubes: the relative roles of oxygen-containing functional groups and graphenic carbon. Langmuir 26, 967–981.

Cho, H.J., Baek, K., Jeon, J.K., Park, S.H., Suh, D.J., Park, Y.K., 2013. Removal characteristics of copper by marine macro-algae-derived chars. Chem. Eng. J. 217, 205–211.

Choi, J.H., Kim, S.S., Ly, H.V., Kim, J., Woo, H.C., 2017. Effects of water-washing Saccharina japonica on fast pyrolysis in a bubbling fluidized-bed reactor. Biomass Bioenergy 98, 112–123.

Choi, Y.K., Choi, T.R., Gurav, R., Bhatia, S.K., Park, Y.L., Kim, H.J., Kan, E., Yang, Y.H., 2020. Adsorption behavior of tetracycline onto *Spirulina* sp. (microalgae)-derived biochars produced at different temperatures. Sci. Total Environ. 710, 136282.

Coronella, C.J., Yan, W., Reza, M.T., Vasquez, V.R. 2012. Method for wet torrefaction of a biomass, Google Patents.

Costa, N.L., Clarke, T.A., Philipp, L.-A., Gescher, J., Louro, R.O., Paquete, C.M., 2018. Electron transfer process in microbial electrochemical technologies: the role of cell-surface exposed conductive proteins. Bioresour. Technol. 255, 308–317.

Cowie, A.L., Downie, A.E., George, B.H., Singh, B.-P., Van Zwieten, L., O'Connell, D., 2012. Is sustainability certification for biochar the answer to environmental risks? Pesq. Agropec. Bras. 47, 637–648.

Crabtree, R.H., 2009. The Organometallic Chemistry of the Transition Metals. Wiley, New York, NY.

Dawood, S., Sen, T.K., Phan, C., 2017. Synthesis and characterization of slow pyrolysis pine cone bio-char in the removal of organic and inorganic pollutants from aqueous solution by adsorption: kinetic, equilibrium, mechanism and thermodynamic. Bioresour. Technol. 246, 76–81.

Du, Z., Li, Y., Wang, X., Wan, Y., Chen, Q., Wang, C., Lin, X., Liu, Y., Chen, P., Ruan, R., 2011. Microwave-assisted pyrolysis of microalgae for biofuel production. Bioresour. Technol. 102, 4890–4896.

Ellison, M.B., de Nys, R., Paul, N.A., Roberts, D.A., 2014. Growth and metal bioconcentration by conspecific freshwater macroalgae cultured in industrial waste water. Peer J. 2, e401.

Ellison, C.R., Hoff, R., Marculescu, C., Boldor, D., 2020. Investigation of microwave-assisted pyrolysis of biomass with char in a rectangular waveguide applicator with built-in phase-shifting. Appl. Energy 259, 114217.

Enaime, G., Baçaoui, A., Yaacoubi, A., Lübken, M., 2020. Biochar for wastewater treatment —conversion technologies and applications. Appl. Sci. 10, 3492.

Ennis, C.J., Evans, A.G., Islam, M., Ralebitso-Senior, T.K., Senior, E., 2012. Biochar: carbon sequestration, land remediation, and impacts on soil microbiology. Crit. Rev. Environ. Sci. Technol. 42 (22), 2311–2364.

Erdinç, N., G€oktürk, S., Tunçay, M., 2010. A study on the adsorption characteristics of an amphiphilic phenothiazine drug on activated charcoal in the presence of surfactants. Colloids Surf. B Biointerfaces 75, 194–203.

Erlach, B., Harder, B., Tsatsaronis, G., 2012. Combined hydrothermal carbonization and gasification of biomass with carbon capture. Energy 45 (1), 329–338.

Fan, Y., Wang, B., Yuan, S.H., Wu, X.H., Chen, J., Wang, L.L., 2010. Adsorptive removal of chloramphenicol from wastewater by NaOH modified bamboo charcoal. Bioresour. Technol. 101 (19), 7661–7664.

Fang, G.D., Gao, J., Liu, C., Dionysiou, D.D., Wang, Y., Zhou, D.M., 2014. Key role of persistent free radicals in hydrogen peroxide activation by biochar: implications to organic contaminant degradation. Environ. Sci. Technol. 48, 1902–1910.

Feng, D., Zhao, Y., Zhang, Y., Sun, S., Meng, S., Guo, Y., 2016. Effects of K and Ca on reforming of model tar compounds with pyrolysis biochars under H_2O or CO_2. Chem. Eng. J. 306, 422–432.

Field, J.L., Keske, C.M.H., Birch, G.L., Defoort, M.W., Cotrufo, M.F., 2013. Distributed biochar and bioenergy coproduction: a regionally specific case study of environmental benefits and economic impacts. Glob. Change Biol. Bioenergy 5, 177–191.

Fierro, V., Mu~niz, G., Basta, A.H., El-Saied, H., Celzard, A., 2010. Rice straw as precursor of activated carbons: activation with ortho-phosphoric acid. J. Hazard. Mater. 181, 27–34.

Fletcher, A.J., Smith, M.A., Heinemeyer, A., Lord, R., Ennis, C.J., Hodgson, E.M., Farrar, K., 2014. Production factors controlling the physical characteristics of biochar derived from phytoremediation willow for agricultural applications. Bioenergy Res. 712 (7 (1)), 371–380.

Francavilla, M., Kamaterou, P., Intini, S., Monteleone, M., Zabaniotou, A., 2015. Cascading microalgae biorefinery: fast pyrolysis of *Dunaliella tertiolecta* lipid extracted-residue. Algal Res. 11, 184–193.

Gao, X., Cheng, H.Y., Valle, I.D., Liu, S., Masiello, C.A., Silberg, J.J., 2016. Charcoal disrupts soil microbial communication through a combination of signal sorption and hydrolysis. ACS Omega 1, 226–233.

Gao, Z., Zhang, Y., Song, N., Li, X., 2017. Biomass-derived renewable carbon materials for electrochemical energy storage. Mater. Res. Lett. 5 (2), 69–88.

Ge, Y., Zhu, S., Chang, J.S., Chao, J., Ho, S.H., 2020. Immobilization of Hg(II) on high-salinity *Spirulina* residue-induced biochar from aqueous solutions: sorption and transformation mechanisms by the dual-mode isotherms. Environ. Pollut. 265, 115087.

Ghidotti, M., Fabbri, D., Homung, A., 2017. Profiles of volatile organic compounds in biochar: insights into process conditions and quality assessment. ACS Sustain. Chem. Eng. 5, 510–517.

Gokulan, R., Avinash, A., Prabhu, G.G., Jegan, J., 2019. Remediation of remazol dyes by biochar derived from *Caulerpa scalpelliformis* - an eco-friendly approach. J. Environ. Chem. Eng. 7, 103297.

Gorby, Y.A., Yanina, S., McLean, J.S., Rosso, K.M., Moyles, D., Dohnalkova, A., Beveridge, T.J., Chang, I.S., Kim, B.H., Kim, K.S., 2006. Electrically conductive bacterial nanowires produced by *Shewanella oneidensis* strain MR-1 and other microorganisms. Proc. Natl. Acad. Sci. U. S. A. 103 (30), 11358–11363.

Graber, E.R., Harel, Y.M., Kolton, M., Cytryn, E., Silber, A., David, D.R., Tsechansky, L., Borenshtein, M., Elad, Y., 2010. Biochar impact on development and productivity of pepper and tomato grown in fertigated soilless media. Plant Soil 337, 481–496.

Grierson, S., Strezov, V., Ellem, G., Mcgregor, R., Herbertson, J., 2009. Thermal characterisation of microalgae under slow pyrolysis conditions. J. Anal. Appl. Pyrol. 85, 118–123.

Gupta, S., Sireesha, S., Sreedhar, I., Patel, C.M., Anitha, K.L., 2020. Latest trends in heavy metal removal from wastewater by biochar based sorbents. J. Water Process Eng. 38, 101561.

Gurav, R., Bhatia, S.K., Choi, T.R., Choi, Y.K., Kim, H.J., Song, H.S., Lee, S.M., Park, S.L., Lee, H.S., Koh, J., Jeon, J.M., Yoon, J.J., Yang, Y.H., 2021. Application of macroalgal biomass derived biochar and bioelectrochemical system with *Shewanella* for the adsorptive removal and biodegradation of toxic azo dye. Chemosphere 264, 128539.

Hammes, K., Smernik, R.J., Skjemstad, J.O., Schmidt, M.W.I., 2008. Characterisation and evaluation of reference materials for black carbon analysis using elemental composition, colour, BET surface area and 13C NMR spectroscopy. Appl. Geochem. 23, 2113–2122.

Hamza, M.F., Lu, S., Salih, K.A.M., Mira, H., Dhmees, A.S., Fujita, T., Wei, Y., Vincent, T., Guibal, E., 2020. As(V) sorption from aqueous solutions using quaternized algal/polyethyleneimine composite beads. Sci. Total Environ. 719, 137396.

Harvey, O.R., Herbert, B.E., Rhue, R.D., Kuo, L.-J., 2011. Metal interactions at the biochar-water interface: energetics and structure-sorption relationships elucidated by flow adsorption microcalorimetry. Environ. Sci. Technol. 45 (13), 5550–5556.

Heilmann, S.M., Davis, H.T., Jader, L.R., Lefebvre, P.A., Sadowsky, M.J., Schendel, F.J., Von Keitz, M.G., Valentas, K.J., 2010. Hydrothermal carbonization of microalgae. Biomass Bioenergy 34 (6), 875–882.

Ho, S.-H., Chen, Y., Yang, Z., Nagarajan, D., Chaang, J., Ren, N., 2017. High-efficiency removal of lead from wastewater by biochar derived from anaerobic digestion sludge. Bioresour. Technol. 246, 142–149.

Ho, S.H., Chen, Y.D., Li, R., Zhang, C., Ge, Y., Cao, G., Ma, M., Duan, X., Wang, S., Ren, N., 2019. N-doped graphitic biochars from C-phycocyanin extracted *Spirulina* residue for catalytic persulfate activation toward nonradical disinfection and organic oxidation. Water Res. 159, 77–86.

Hong, Y., Chen, W., Luo, X., Pang, C., Lester, E., Wu, T., 2017. Microwave-enhanced pyrolysis of macroalgae and microalgae for syngas production. Bioresour. Technol. 237, 47–56.

Huang, Q., Liu, M., Wan, Q., Jiang, R., Mao, L., Zen, G., Huang, H., Deng, F., Zhang, X., Wei, Y., 2017. Preparation of polymeric silica composites through polydopamine-mediated surface initiated ATRP for highly efficient removal of environmental pollutants. Mater. Chem. Phys. 193, 501–511.

Huggins, T., Wang, H., Kearns, J., Jenkins, P., Ren, Z.J., 2014. Biochar as a sustainable electrode material for electricity production in microbial fuel cells. Bioresour. Technol. 157, 114–119.

Hung, C.M., Huang, C.P., Hsieh, S.L., Tsai, M.L., Chen, C.W., Dong, C.D., 2020. Biochar derived from red algae for efficient remediation of 4-nonylphenol from marine sediments. Chemosphere 254, 126916.

Inyang, M., Gao, B., Pullammanappallil, P., Ding, W., Zimmerman, A.R., 2010. Biochar from anaerobically digested sugarcane bagasse. Bioresour. Technol. 101, 8868–8872.

Inyang, M., Gao, B., Ding, W., Pullammanappallil, P., Zimmerman, A.R., Cao, X., 2011. Enhanced lead sorption by biochar derived from anaerobically digested sugarcane bagasse. Sep. Sci. Technol. 46, 1950–1956.

Inyang, M., Gao, B., Yao, Y., Xue, Y., Zimmerman, A.R., Pullammanappallil, P., Cao, X., 2012. Removal of heavy metals from aqueous solution by biochars derived from anaerobically digested biomass. Bioresour. Technol. 110, 50–56.

Inyang, M.D., Gao, B., Zimmerman, A., Zhou, Y., Cao, X., 2014. Sorption and cosorption of lead and sulfapyridine on carbon nanotube-modified biochars. Environ. Sci. Pollut. Res. 22, 1868–1876.

Inyang, M., Gao, B., Zimmerman, A., Zhou, Y., Cao, X., 2015. Sorption and cosorption of lead and sulfapyridine on carbon nanotube-modified biochars. Environ. Sci. Pollut. Res. 22, 1868–1876.

Inyang, M., Gao, B., Yao, Y., Xue, Y.W., Zimmerman, A., Mosa, A., Pullammanappallil, P., Yong, S.O., Cao, X.D., 2016. A review of biochar as a low-cost adsorbent for aqueous heavy metal removal. Crit. Rev. Environ. Sci. Technol. 46 (4), 406–433.

Jimenez-Cordero, D., Heras, F., Alonso-Morales, N., Gilarranz, M.A., Rodriguez, J.J., 2015. Ozone as oxidation agent in cyclic activation of biochar. Fuel Process. Technol. 139, 42–48.

Jin, H., Hanif, M.U., Capareda, S., Chang, Z., Huang, H., Ai, Y., 2016. Copper(II) removal potential from aqueous solution by pyrolysis biochar derived from anaerobically digested algae-dairy-manure and effect of KOH activation. J. Environ. Chem. Eng. 4, 365–372.

Jindo, K., Mizumoto, H., Sawada, Y., Sanchez-Monedero, M.A., Sonoki, T., 2014. Physical and chemical characterization of biochars derived from different agricultural residues. Biogeosciences 11 (23), 6613–6621.

Jing, X.-R., Wang, Y.-Y., Liu, W.-J., Wang, Y.-K., Jiang, H., 2014. Enhanced adsorption performance of tetracycline in aqueous solutions by methanol-modified biochar. Chem. Eng. J. 248, 168–174.

Johansson, C.L., Paul, N.A., de Nys, R., Roberts, D.A., 2016. Simultaneous biosorption of selenium, arsenic and molybdenum with modified algal-based biochars. J. Environ. Manag. 165, 117–123.

Joseph, S., Graber, E.R., Chia, C., Munroe, P., Donne, S., Thomas, T., 2013. Shifting paradigms: development of high-efficiency biochar fertilizers based on nano-structures and soluble components. Carbon Manag. 4, 323–343.

Jung, K.-W., Jeong, T.-U., Kang, H.-J., Ahn, K.-H., 2016. Characteristics of biochar derived from marine macroalgae and fabrication of granular biochar by entrapment in calcium-alginate beads for phosphate removal from aqueous solution. Bioresour. Technol. 211, 108–116.

Kah, M., Sigmund, G., Xiao, F., Hofmann, T., 2017. Sorption of ionizable and ionic organic compounds to biochar, activated carbon and other carbonaceous materials. Water Res. 124, 673–692.

Karthik, V., Senthil Kumar, P., Vo, Dai-Viet N., Sindhu, J., Sneka, D., Subhashini, B., Saravanan, K., Jeyanthi, J., 2020. Hydrothermal production of algal biochar for environmental and fertilizer applications: a review. Environ. Chem. Lett. https://doi.org/10.1007/s10311-020-01139-x.

Kastner, J.R., Miller, J., Geller, D.P., Locklin, J., Keith, L.H., Johnson, T., 2012. Catalytic esterification of fatty acids using solid acid catalysts generated from biochar and activated carbon. Catal. Today 190, 122–132.

Keiluweit, M., Kleber, M., 2009. Molecular-level interactions in soils and sediments: the role of aromatic pi-systems. Environ. Sci. Technol. 43, 3421–3429.

Khodadad, C.L.M., Zimmerman, A.R., Green, S.J., Uthandi, S., Foster, J.S., 2011. Taxa-specific changes in soil microbial community composition induced by pyrogenic carbon amendments. Soil Biol. Biochem. 43 (2), 385–392.

Kim, W.-K., Shim, T., Kim, Y.-S., Hyun, S., Ryu, C., Park, Y.-K., Jung, J., 2013. Characterization of cadmium removal from aqueous solution by biochar produced from a giant *Miscanthus* at different pyrolytic temperatures. Bioresour. Technol. 138, 266–270.

Kim, B., Lee, H.W., Park, S.H., Baek, K., Jeon, J., Cho, H.J., Jung, S., Kim, S.C., Park, Y., 2016. Removal of Cu^{2+} by biochars derived from green macroalgae. Environ. Sci. Pollut. Res. 23, 985–994.

Koga, N., Shimoda, S., Iwata, Y., 2017. Biochar impacts on crop productivity and greenhouse gas emissions from an andosol. J. Environ. Qual. 46, 27–35.

Kołtowski, M., Charmas, B., Skubiszewska-Zięba, J., Oleszczuk, P., 2017. Effect of biochar activation by different methods on toxicity of soil contaminated by industrial activity. Ecotoxicol. Environ. Saf. 136, 119–125.

Kong, L.L., Liu, W.T., Zhou, Q.X., 2014. Biochar: an effective amendment for remediating contaminated soil. Rev. Environ. Contam. Toxicol. 228, 83–99.

Koutcheiko, S., Vorontsov, V., 2013. Activated carbon derived from wood biochar and its application in supercapacitors. J. Biobased Mater. Bio. 7, 733–740.

Kumar, S., Loganathan, V.A., Gupta, R.B., Barnett, M.O., 2011. An assessment of U(VI) removal from groundwater using biochar produced from hydrothermal carbonization. J. Environ. Manag. 92, 2504–2512.

Kumar, G., Shobana, S., Chen, W.-H., Bach, Q.-V., Kim, S.-H., Atabani, A.E., Chang, J.-S., 2017. A review of thermochemical conversion of microalgal biomass for biofuels: chemistry and processes. Green Chem. 19 (1), 44–67.

Kumar, A., Kumar, A., Sharma, G., Al-Muhtaseb, A.H., Naushad, M., Ghfar, A.A., Guo, C., Stadler, F.J., 2018. Biochar-templated g-C$_3$N$_4$/Bi$_2$O$_2$CO$_3$/CoFe$_2$O$_4$ nano-assembly for visible and solar assisted photo-degradation of paraquat, nitrophenol reduction and CO$_2$ conversion. Chem. Eng. J. 339, 393–410.

Laine, J., Simoni, S., Calles, R., 1991. Preparation of activated carbon from coconut shell in a small scale concurrent flow rotary kiln. Chem. Eng. Commun. 99, 15–23.

Lalhmunsiama, Gupta, P.L., Jung, H., Tiwari, D., Kong, S.H., Lee, S.M., 2017. Insight into the mechanism of Cd (II) and Pb (II) removal by sustainable magnetic biosorbent precursor to *Chlorella vulgaris*. J. Taiwan Inst. Chem. E 71, 206–213.

Lattao, C., Cao, X., Mao, J., Schmidt-Rohr, K., Pignatello, J.J., 2014. Influence of molecular structure and adsorbent properties on sorption of organic compounds to a temperature series of wood chars. Environ. Sci. Technol. 48, 4790–4798.

Lawton, R.J., de Nys, R., Paul, N.A., 2013. Selecting reliable and robust freshwater macroalgae for biomass applications. PLoS One 8, e64168.

Lee, X.J., Ong, H.C., Gan, Y.Y., Chen, W.H., Mahila, T.M.I., 2020. State of art review on conventional and advanced pyrolysis of macroalgae and microalgae for biochar, bio-oil and bio-syngas production. Energy Convers. Manag. 210, 112707.

Lehmann, J., Rillig, M., Thies, J., Masiello, C.A., Hockaday, W.C., Crowley, D., 2011. Biochar effects on soil biota-a review. Soil Biol. Biochem. 43, 1812–1836.

Li, J.-H., Lv, G.-H., Bai, W.-B., Liu, Q., Zhang, Y.-C., Song, J.-Q., 2014. Modification and use of biochar from wheat straw (*Triticum aestivum* L.) for nitrate and phosphate removal from water. Desalination Water Treat. 1–13.

Li, X.P., Wang, C.B., Zhang, J.G., Liu, B., Liu, J.P., Chen, G.Y., 2018. Application of biochar in removal of organics and heavy metals from water. Acta Pet. Sin. 34, 1047–1056.

Liang, B., Lehmann, J., Solomon, D., Kinyangi, J., Grossman, J., O'Neill, B., Skjemstad, J., Thies, J., Luizao, F., Petersen, J., 2006. Black carbon increases cation exchange capacity in soils. Soil Sci. Soc. Am. J. 70, 1719–1730.

Liang, B., Lehmann, J., Solomon, D., Sohi, S., Thies, J.E., Skjemstad, J.O., Luizão, F.J., Engelhard, M.H., Neves, E.G., Wirick, S., 2008. Stability of biomass-derived black carbon in soils. Geochim. Cosmochim. Acta 72, 6069–6078.

Liao, S.H., Pan, B., Li, H., Zhang, D., Xing, B.S., 2014. Detecting free radicals in biochars and determining their ability to inhibit the germination and growth of corn, wheat and rice seedlings. Environ. Sci. Technol. 48, 8581–8587.

Libra, J.A., Ro, K.S., Kammann, C., Funke, A., Berge, N.D., Neubauer, Y., Titirici, M.-M., Fühner, C., Bens, O., Kern, J., 2011. Hydrothermal carbonization of biomass residuals: a comparative review of the chemistry, processes and applications of wet and dry pyrolysis. Biofuels 2 (1), 71–106.

Lima, I.M., Boateng, A.A., Klasson, K.T., 2010. Physicochemical and adsorptive properties of fast-pyrolysis bio-chars and their steam activated counterparts. J. Chem. Technol. Biotechnol. 85, 1515–1521.

Lin, Y., Munroe, P., Joseph, S., Henderson, R., Ziolkowski, A., 2012. Water extractable organic carbon in untreated and chemical treated biochars. Chemosphere 87, 151–157.

Lin, L., Qiu, W., Wang, D., Huang, Q., Song, Z., Chau, H.W., 2017. Arsenic removal in aqueous solution by a novel Fe-Mn modified biochar composite: characterization and mechanism. Ecotoxicol. Environ. Saf. 144, 514–521.

Liu, Z., Zhang, F., 2009. Removal of lead from water using biochars prepared from hydrothermal liquefaction of biomass. J. Hazard. Mater. 167, 933–939.

Liu, J., He, L., Dong, F., Hudson-Edwards, K.A., 2016. The role of nano-sized manganese coatings on bone char in removing arsenic(V) from solution: implications for permeable reactive barrier technologies. Chemosphere 153, 146–154.

Liu, Z., Yang, W., Xu, W., Liu, Y., 2018. Removal of elemental mercury by bio-chars derived from seaweed impregnated with potassium iodine. Chem. Eng. J. 339, 468–478.

Llanos, J., Williams, P.M., Cheng, S., Rogers, D., Wright, C., Perez, A., Canizares, P., 2010. Characterization of a ceramic ultrafiltration membrane in different operational states after its use in a heavy-metal ion removal process. Water Res. 44, 3522–3530.

Lu, J., Zhang, C., Wu, J., Luo, Y., 2017. Adsorptive removal of bisphenol A using N-doped biochar made of *Ulva prolifera*. Water Air Soil Pollut. 228, 327.

Lu, J., Zhang, C., Wu, J., 2020. One-pot synthesis of magnetic algal carbon/sulfidated nanoscale zerovalent iron composites for removal of bromated disinfection by-product. Chemosphere 250, 126257.

Luo, C.H., Lü, F., Shao, L.M., He, P.J., 2015. Application of eco-compatible biochar in anaerobic digestion to relieve acid stress and promote the selective colonization of functional microbes. Water Res. 68, 710–718.

Lyu, H., He, Y., Hecker, M., Liu, Q., Jones, P.D., Codling, G., Giesy, J.P., 2016. Effect of pyrolysis temperature on potential toxicity of biochar if applied to the environment. Environ. Pollut. 218, 1–7.

Lyu, H., Gao, B., He, F., Zimmerman, A., Ding, C., Huang, H., Tang, J., 2018. Effects of ball milling on the physicochemical and sorptive properties of biochar: experimental observations and governing mechanisms. Environ. Pollut. 233, 54–63.

Maddi, B., Viamajala, S., Varanasi, S., 2011. Comparative study of pyrolysis of algal biomass from natural lake blooms with lignocellulosic biomass. Bioresour. Technol. 102 (23), 11018–11026.

Malaviya, P., Singh, A., 2011. Physicochemical technologies for remediation of chromium-containing waters and wastewaters. Crit. Rev. Environ. Sci. Technol. 41 (12), 1111–1172.

Malaviya, P., Singh, A., 2016. Bioremediation of chromium solutions and chromium containing wastewaters. Crit. Rev. Microbiol. 42, 607–633.

Malaviya, P., Singh, A., Anderson, T.A., 2020. Aquatic phytoremediation strategies for chromium removal. Rev. Environ. Sci. Biotechnol. 19, 897–944.

Marcilla, A., Catala, L., García-Quesada, J.C., Valdes, F., Hernandez, M., 2013. A review of thermochemical conversion of microalgae. Renew. Sust. Energ. Rev. 27, 11–19.

Menendez, J.A., Domıenguez, A., Inguanzo, M., Pis, J.J., 2004. Microwave pyrolysis of sewage sludge: analysis of the gas fraction. J. Anal. Appl. Pyrol. 71, 657–667.

Meng, J., Feng, X., Dai, Z., Liu, X., Wu, J., Xu, J., 2014. Adsorption characteristics of Cu(II) from aqueous solution onto biochar derived from swine manure. Environ. Sci. Pollut. Res. 21, 7035–7046.

Metz, L.A., Meruva, N.K., Morgan, S.L., Goode, S.R., 2004. UV laser pyrolysis fast gas chromatography/time-of-flight mass spectrometry for rapid characterization of synthetic polymers: optimization of instrumental parameters. J. Anal. Appl. 71, 327–341.

Miao, X., Wu, Q., Yang, C., 2004. Fast pyrolysis of microalgae to produce renewable fuels. J. Anal. Appl. Pyrol. 71 (2), 855–863.

Miao, C., Chakraborty, M., Chen, S., 2012. Impact of reaction conditions on the simultaneous production of polysaccharides and bio-oil from heterotrophically grown *Chlorella sorokiniana* by a unique sequential hydrothermal liquefaction process. Bioresour. Technol. 110, 617–627.

Michalak, I., Basladynska, S., Mokrzycki, J., Rutkowski, P., 2019. Biochar from a freshwater macroalga as a potential biosorbent for wastewater treatment. Water 11, 1390.

Mishra, A., Medhi, K., Malaviya, P., Thakur, I.S., 2019. Omics approaches for microalgal applications: prospects and challenges. Bioresour. Technol. 291, 121890.

Mochidzuki, K., Soutric, F., Tadokoro, K., Antal, M.J., Toth, M., Zelei, B., Várhegyi, G., 2003. Electrical and physical properties of carbonized charcoals. Ind. Eng. Chem. Res. 42, 5140–5151.

Mohamed, B.A., Ellis, N., Kim, C.S., Bi, X., Emam, A.E.-R., 2016. Engineered biochar from microwave-assisted catalytic pyrolysis of switchgrass for increasing waterholding capacity and fertility of sandy soil. Sci. Total Environ. 566–567, 387–397.

Mohan, D., Sarswat, A., Ok, Y., Pittman Jr., C.U., 2014a. Organic and inorganic contaminants removal from water with biochar, a renewable, low cost and sustainable adsorbent: a critical review. Bioresour. Technol. 160, 191–202.

Mohan, D., Kumar, H., Sarswat, A., Alexandre-Franco, M., Pittman Jr., C.U., 2014b. Cadmium and lead remediation using magnetic oak wood and oak bark fast pyrolysis bio-chars. Chem. Eng. J. 236, 513–528.

Molina, M., Zaelke, D., Sarma, K.M., Andersen, S.O., Ramanathan, V., Kaniaru, D., 2009. Reducing abrupt climate change risk using the Montreal protocol and other regulatory actions to complement cuts in CO_2 emissions. Proc. Natl. Acad. Sci. 106 (49), 20616–20621.

Mukherjee, A., Zimmerman, A.R., Harris, W., 2011. Surface chemistry variations among a series of laboratory-produced biochars. Geoderma 163, 247–255.

Mukome, F.N., Zhang, X., Silva, L.C., Six, J., Parikh, S.J., 2013. Use of chemical and physical characteristics to investigate trends in biochar feedstocks. J. Agric. Food Chem. 61 (9), 2196–2204.

Muneer, B., Zeeshan, M., Qaisar, S., Razzaq, M., Iftikhar, H., 2019. Influence of in-situ and ex-situ HZSM-5 catalyst on co-pyrolysis of corn stalk and polystyrene with a focus on liquid yield and quality. J. Clean. Prod. 237, 117762.

Mwangi, J.K., Lee, W.J., Whang, L.M., Wu, T.S., Chen, W.H., Chang, J.S., Chen, C.Y., Chen, C.L., 2015. Microalgae oil: algae cultivation and harvest, algae residue torrefaction and diesel engine emissions tests. Aerosol Air Qual. Res. 81–98.

Nagappan, S., Devendran, S., Tsai, P.-C., Dinakaran, S., Dahms, H.-U., Ponnusamy, V.K., 2019. Passive cell disruption lipid extraction methods of microalgae for biofuel production—a review. Fuel 252, 699–709.

Nautiyal, P., Subramanian, K.A., Dastidar, M.G., 2016. Adsorptive removal of dye using biochar derived from residual algae after in-situ transesterification: alternate use of waste of biodiesel industry. J. Environ. Manag. 182, 187–197.

Neveux, N., Yuen, A.K.L., Jazrawi, C., Magnusson, M., Haynes, B.S., Masters, A.F., Montoya, A., Paul, N.A., Maschmeyer, T., de Nys, R., 2014. Biocrude yield and productivity from the hydrothermal liquefaction of marine and freshwater green macroalgae. Bioresour. Technol. 155, 334–341.

Nhuchhen, D.R., Basu, P., Acharya, B., 2014. A comprehensive review on biomass torrefaction. Int. J. Renew. Energ. Biofuels 2014, 1–56.

Niu, Q., Luo, J., Xia, Y., Sun, S., Chen, Q., 2017. Surface modification of bio-char by dielectric barrier discharge plasma for Hg0 removal. Fuel Process. Technol. 156, 310–316.

Norouzi, O., Tavasoli, A., Jafarian, S., Esmailpour, S., 2017. Catalytic upgrading of bio-products derived from pyrolysis of red macroalgae *Gracilaria gracilis* with a promising novel micro/mesoporous catalyst. Bioresour. Technol. 243, 1–8.

Novak, J.M., Isabel, L., Xing, B., Gaskin, J.W., Steiner, C., Das, K.C., Ahmedna, M., Rehrah, D., Watts, D.W., Busscher, W.J., Schomberg, H., 2009. Characterization of designer biochar produced at different temperatures and their effects on a loamy sand. Ann. Environ. Sci. 3, 195–206.

Ok, Y.S., Chang, S.X., Gao, B., Chung, H.-J., 2015. SMART biochar technology-a shifting paradigm towards advanced materials and healthcare research. Environ. Technol. Inno. 4, 206–209.

Paethanom, A., Yoshikawa, K., 2012. Influence of pyrolysis temperature on rice husk 831 char characteristics and its tar adsorption capability. Energies 5 (12), 4941–4951.

Palanisamy, M., Mukund, S., Sivakumar, U., Karthikeyan, Sivasubramanian, V., 2017. Biochar production from micro algal biomass of *Chlorella vulgaris*. PHYKOS. 47 (1), 99–104.

Park, J.H., Choppala, G.K., Bolan, N.S., Chung, J.W., Chuasavathi, T., 2011. Biochar reduces the bioavailability and phytotoxicity of heavy metals. Plant Soil 348, 1–13.

Park, S.H., Cho, H.J., Ryu, C., Park, Y.K., 2016. Removal of copper(II) in aqueous solution using pyrolytic biochars derived from red macroalga *Porphyra tenera*. J. Ind. Eng. Chem. 36, 314–319.

Paz-Ferreiro, J., Fu, S., Mendez, A., Gasco, G., 2014. Interactive effects of biochar and the earthworm *Pontoscolex corethrurus* on plant productivity and soil enzyme activities. J. Soils Sedim. 14, 483–494.

Pignatello, J.J., 2011. Interactions of anthropogenic organic chemicals with natural organic matter and black carbon in environmental particles. Biophysico-Chemical Processes of Anthropogenic Organic Compounds in Environmental Systems. JohnWiley Sons, Inc., Hoboken, NJ, USA, pp. 1–50.

Placido, J., Bustamante-Lopez, S., Meissner, K.E., Kelly, D.E., Kelly, S.L., 2019. Microalgae biochar-derived carbon dots and their application in heavy metal sensing in aqueous systems. Sci. Total Environ. 656, 531–539.

Poo, K.M., Son, E.B., Chang, J.S., Ren, X., Chae, K.J., 2018. Biochars derived from wasted marine macro-algae (*Saccharina japonica* and *Sargassum fusiforme*) and their potential for heavy metal removal in aqueous solution. J. Environ. Manag. 206, 364–372.

Pourhosseini, S.E.M., Norouzi, O., Naderi, H.R., 2017. Study of micro/macro ordered porous carbon with olive-shaped structure derived from *Cladophora glomerata* macroalgae as efficient working electrodes of supercapacitors. Biomass Bioenerg. 107, 287–298.

Pourhosseini, S.E.M., Norouzi, O., Salimi, P., Naderi, H.R., 2018. Synthesis of a novel interconnected 3D pore network algal biochar constituting iron nanoparticles derived from a harmful marine biomass as high-performance asymmetric supercapacitor electrodes. ACS Sustain. Chem. Eng. 4746–4758.

Prado, A., Berenguer, R., Esteve-Núñez, A., 2019. Electroactive biochar outperforms highly conductive carbon materials for biodegrading pollutants by enhancing microbial extracellular electron transfer. Carbon N. Y. 146, 597–609.

Qi, Y., Ge, B., Zhang, Y., Jiang, B., Wang, C., Akram, M., Xu, X., 2020. Three-dimensional porous graphene-like biochar derived from *Enteromorpha* as a persulfate activator for sulfamethoxazole degradation: role of graphitic N and radicals transformation. J. Hazard. Mater. 399, 123039.

Qian, K., Kumar, A., Patil, K., Bellmer, D., Wang, D., Yuan, W., Huhnke, R.L., 2013. Effects of biomass feedstocks and gasification conditions on the physiochemical properties of char. Energies 6 (8), 3972–3986.

Qian, K., Kumar, A., Zhang, H., Bellmer, D., Huhnke, R., 2015. Recent advances in utilization of biochar. Renew. Sust. Energ. Rev. 42, 1055–1064.

Qian, L.B., Zhang, W.Y., Yan, J.C., Han, L., Chen, Y., Ouyang, D., Chen, M.F., 2017. Nanoscale zero-valent iron supported by biochars produced at different temperatures: synthesis mechanism and effect on Cr(VI) removal. Environ. Pollut. 223, 153–160.

Qiao, K.L., Tian, W.J., Bai, J., Dong, J., Zhao, J., Gong, X.X., Liu, S.H., 2017. Preparation of biochar from *Enteromorpha prolifera* and its use for the removal of polycyclic aromatic hydrocarbons (PAHs) from aqueous solution. Ecotoxicol. Environ. Saf. 149, 80–87.

Quilliam, R.S., Glanville, H.C., Wade, S.C., Jones, D.L., 2013. Life in the 'charosphere' – does biochar in agricultural soil provide a significant habitat for microorganisms? Soil Biol. Biochem. 65, 287–293.

Rajapaksha, A.U., Vithanage, M., Weerasooriya, R., Dissanayake, C.B., 2012. Surface complexation of nickel on iron and aluminum oxides: a comparative study with single and dual site clays. Colloids Surf. A Physicochem. Eng. Aspects 405, 79–87.

Rajapaksha, A.U., Vithanage, M., Zhang, M., Ahmad, M., Mohan, D., Chang, S.X., Ok, Y.S., 2014. Pyrolysis condition affected sulfamethazine sorption by tea waste biochars. Bioresour. Technol. 166, 303–308.

Rajapaksha, A.U., Vithanage, M., Ahmad, M., Seo, D.C., Cho, J.S., Lee, S.E., Lee, S.S., Ok, Y.S., 2015. Enhanced sulfamethazine removal by steam-activated invasive plant-derived biochar. J. Hazard. Mater. 290, 43–50.

Rajapaksha, A.U., Chen, S.S., Tsang, D.C., Zhang, M., Vithanage, M., Mandal, S., Gao, B., Bolan, N.S., Ok, Y.S., 2016. Engineered/designer biochar for contaminant removal/immobilization from soil and water: potential and implication of biochar modification. Chemosphere 148, 276–291.

Ramírez-Vargas, C.A., Prado, A., Arias, C.A., Carvalho, P.N., Esteve-Núñez, A., Brix, H., 2018. Microbial electrochemical technologies for wastewater treatment: principles and evolution from microbial fuel cells to bioelectrochemical-based constructed wetlands. Water 10, 1128.

Rathinam, A., Rao, J.R., Nair, B.U., 2011. Adsorption of phenol onto activated carbon from seaweed: determination of the optimal experimental parameters using factorial design. J. Taiwan Inst. Chem. E 42, 952–956.

Raymundo-Pinero, E., Leroux, F., Beguin, F., 2006. A high-performance carbon for supercapacitors obtained by carbonization of a seaweed biopolymer. Adv. Mater. 18, 1877–1882.

Roberts, D.A., de Nys, R., Paul, N.A., 2013. The effect of CO_2 on algal growth in industrial waste water for bioenergy and bioremediation applications. PLoS One 8, e81631.

Roberts, D.A., Paul, N.A., Cole, A.J., de Nys, R., 2015a. From waste water treatment to land management: conversion of biomass to biochar for soil amelioration and the fortification of crops with essential trace elements. J. Environ. Manag. 157, 60–68.

Roberts, D.A., Cole, A.J., Paul, N.A., de Nys, R., 2015b. Algal biochar enhances the revegetation of stockpiled mine soils with native grass. J. Environ. Manag. 161, 173–180.

Roberts, D.A., Paul, N.A., Dworjanyn, S.A., Bird, M.I., de Nys, R., 2015c. Biochar from commercially cultivated seaweed for soil amelioration. Sci. Rep. 5, 9665.

Roberts, D.A., Paul, N.A., Bird, M.I., de Nys, R., 2015d. Bioremediation for coal-fired power stations using macroalgae. J. Environ. Manag. 153, 25–32.

Roberts, D.A., Paul, N.A., Dworjanyn, S.A., Hu, Y., Bird, M.I., de Nys, R., 2015e. *Gracilaria* waste biomass (sampah rumput laut) as a substrate for selenium bioremediation. J. Appl. Phycol. 27, 611–620.

Ronsse, F., van Hecke, S., Dickinson, D., Prins, W., 2013. Production and characterization of slow pyrolysis biochar: influence of feedstock type and pyrolysis conditions. GCB Bioenergy 5 (2), 104–115.

Rosales, E., Meijide, J., Pazos, M., Sanroman, M.A., 2017. Challenges and recent advances in biochar as lowcost biosorbent: from batch assays to continuous-flow systems. Bioresour. Technol. 246, 176–192.

Rufford, T.E., Hulicova-Jurcakova, D., Zhu, Z., Lu, G.Q., 2008. Nanoporous carbon electrode from waste coffee beans for high performance supercapacitors. Electrochem. Commun. 10, 1594–1597.

Ryu, Y.J., Kim, Z.H., Lee, S.G., Yang, J.H., Shin, H.Y., Lee, C.G., 2018. Development of carbon-based solid acid catalysts using a lipid-extracted alga, *Dunaliella tertiolecta*, for esterification. J. Microbiol. Biotechnol. 28, 732–738.

Safari, F., Norouzi, O., Tavasoli, A., 2016. Hydrothermal gasification of *Cladophora glomerata* macroalgae over its hydrochar as a catalyst for hydrogen-rich gas production. Bioresour. Technol. 222, 232–241.

Salimi, P., Javadian, S., Norouzi, O., Gharibi, H., 2017. Turning an environmental problem into an opportunity: potential use of biochar derived from a harmful marine biomass named *Cladophora glomerata* as anode electrode for Li-ion batteries. Environ. Sci. Pollut. Res. 24 (36), 27974–27984.

Samsudin, M.H., Hassan, M.A., Idris, J., Ramli, N., Yusoff, M.Z.M., Ibrahim, I., Othman, M.R., Ali, A.A.M., Shirai, Y., 2019. A one-step self-sustained low temperature carbonization of coconut shell biomass produced a high specific surface area biochar-derived nano-adsorbent. Waste Manag. Res. 37, 551–555.

Santhanalakshmi, J., Balaji, S., 1996. Adsorption studies of nonionic surfactants on charcoal and alumina in aromatic solvents. J. Colloid Interface Sci. 179, 517–521.

Schievano, A., Berenguer, R., Goglio, A., Bocchi, S., Marzorati, S., Rago, L., Louro, R.O., Paquete, C., Esteve-Núñez, A., 2019. Electroactive biochar for large-scale environmental applications of microbial electrochemistry. ACS Sustain. Chem. Eng. 7 (22), 18198–18212.

Sekar, M., Mathimani, T., Alagumalai, A., Chi, N.T.L., Duc, P.A., Bhatia, S.K., Brindhadevi, K., Pugazhendhi, A., 2021. A review on the pyrolysis of algal biomass for biochar and bio-oil – bottlenecks and scope. Fuel 283, 119190.

Setter, C., Silva, F.T.M., Assis, M.R., Ataíde, C.H., Trugilho, P.F., Oliveira, T.J.P., 2020. Slow pyrolysis of coffee husk briquettes: characterization of the solid and liquid fractions. Fuel 261, 116420.

Sevda, S., Garlapati, V.K., Sharma, S., Bhattacharya, S., Mishra, S., Sreekrishnan, T.R., Pant, D., 2019. Microalgae at niches of bioelectrochemical systems: a new platform for sustainable energy production coupled industrial effluent treatment. Bioresour. Technol. Rep. 7, 100290.

Shafeeyan, M.S., Daud, W.M.A.W., Houshmand, A., Shamiri, A., 2010. A review on surface modification of activated carbon for carbon dioxide adsorption. J. Anal. Appl. Pyrolysis 89, 143–151.

Sharma, R., Malaviya, P., 2021. Management of stormwater pollution using green infrastructure: the role of rain gardens. WIREs Water https://doi.org/10.1002/wat2.1507.

Sharma, G., Bhogal, S., Gupta, V.K., Agarwal, S., Kumar, A., Pathania, D., Mola, G.T., 2019. Algal biochar reinforced trimetallic nanocomposite as adsorptional/photocatalyst for remediation of malachite green from aqueous medium. J. Mol. Liq. 275, 499–509.

Shen, Y., Zhao, P., Shao, Q., Ma, D., Takahashi, F., Yoshikawa, K., 2014. In-situ catalytic conversion of tar using rice husk char-supported nickel-iron catalysts for biomass pyrolysis/gasification. Appl. Catal. B Environ. 152–153, 140–151.

Shen, Y., Li, H., Zhu, W., Ho, S.H., Yuan, W., Chen, J., Xie, Y., 2017. Microalgal-biochar immobilized complex: a novel efficient biosorbent for cadmium removal from aqueous solution. Bioresour. Technol. 244, 1031–1038.

Shukla, S.P., Gita, S., Bharti, V.S., Bhuvaneswari, G.R., Wikramasinghe, W.A.A.D.L., 2017. Atmospheric carbon sequestration through microalgae: status, prospects, and challenges. Agro-Environmental Sustainability. Springer, pp. 219–235.

Simão, B.L., Santana Júnior, J.A., Chagas, B.M.E., Cardoso, C.R., Ataíde, C.H., 2018. Pyrolysis of *Spirulina maxima*: kinetic modeling and selectivity for aromatic hydrocarbons. Algal Res. 32, 221–232.

Singh, A., Malaviya, P., 2019. Chromium phytoaccumulation and its impact on growth and photosynthetic pigments of *Spirodela polyrrhiza* (L.) Schleid. on exposure to tannery effluent. J. Environ. Sustain. 2, 157–166.

Singh, A., Vyas, D., Malaviya, P., 2016. Two-stage phyto-microremediation of tannery effluent by *Spirodela polyrrhiza* (L.) Schleid. and chromium resistant bacteria. Bioresour. Technol. 216, 883–893.

Sizmur, T., Quilliam, R., Puga, A.P., Moreno-Jiménez, E., Beesley, L., Gomez-Eyles, J.L., 2016. Application of biochar for soil remediation. Agricultural and Environmental Applications of Biochar: Advances and Barriers. 63. SSSA Special Publications, pp. 295–324.

Son, E.-B., Poo, K.-M., Chang, J.-S., Chae, K.-J., 2018. Heavy metal removal from aqueous solutions using engineered magnetic biochars derived from waste marine macro-algal biomass. Sci. Total Environ. 615, 161–168.

Spokas, K.A., Novak, J.M., Stewart, C.E., Cantrell, K.B., Uchimiya, M., DuSaire, M.G., Ro, K.S., 2011. Qualitative analysis of volatile organic compounds on biochar. Chemosphere 85, 869–882.

Stavropoulos, G.G., Samaras, P., Sakellaropoulos, G.P., 2008. Effect of activated carbons modification on porosity, surface structure and phenol adsorption. J. Hazard. Mater. 151, 414–421.

Subramanian, V., Luo, C., Stephan, A., Nahm, K., Thomas, S., Wei, B., 2007. Supercapacitors from activated carbon derived from banana fibers. J. Phys. Chem.C. 111, 7527–7531.

Sun, K., Jian-chun, J., Dan-dan, C., 2011. Preparation of activated carbon with highly developed mesoporous structure from *Camellia oleifera* shell through water vapor gasification and phosphoric acid modification. Biomass Bioenergy 35, 3643–3647.

Sun, L., Chen, D., Wan, S., Yu, Z., 2015a. Performance, kinetics, and equilibrium of methylene blue adsorption on biochar derived from eucalyptus saw dust modified with citric, tartaric, and acetic acids. Bioresour. Technol. 198, 300–308.

Sun, D., Meng, J., Liang, H., Yang, E., Huang, Y., Chen, W., Jiang, L., Lan, Y., Zhang, W., Gao, J., 2015b. Effect of volatile organic compounds absorbed to fresh biochar on survival of *Bacillus mucilaginosus* and structure of soil microbial communities. J. Soils Sedim. 15, 271–281.

Sun, H., Lu, H., Chu, L., Shao, H., Shi, W., 2017. Biochar applied with appropriate rates can reduce N leaching, keep N retention and not increase NH_3 volatilization in a coastal saline soil. Sci. Total Environ. 575, 820–825.

Sun, X., Atiyeh, H.K., Li, M., Chen, Y., 2020. Biochar facilitated bioprocessing and biorefinery for productions of biofuel and chemicals: a review. Bioresour. Technol. 295, 122252.

Tag, A.T., Duman, G., Ucar, S., Yanik, J., 2016. Effects of feedstock type and pyrolysis temperature on potential applications of biochar. J. Anal. Appl. Pyrol. 120, 200–206.

Taghavi, S., Norouzi, O., Tavasoli, A., Di Maria, F., Signoretto, M., Menegazzo, F., Michele, A.D., 2018. Catalytic conversion of Venice lagoon brown marine algae for producing hydrogen-rich gas and valuable biochemical using algal biochar and Ni/SBA-15 catalyst. Int. J. Hydrog. Energy 43, 19918–19929.

Tan, X., Liu, Y., Zeng, G., Wang, X., Hu, X., Gu, Y., Yang, Z., 2015. Application of biochar for the removal of pollutants from aqueous solutions. Chemosphere 125, 70–85.

Tan, X.F., Liu, Y.-G., Gu, Y.-L., Xu, Y., Zeng, G.M., Hu, X.Z., Liu, S.B., Wang, X., Liu, S.M., Li, J., 2016. Biochar-based nano-composites for the decontamination of wastewater: a review. Bioresour. Technol. 212, 318–333.

Tan, X.-F., Liu, S.-B., Liu, Y.-G., Gu, Y.-L., Zeng, G.-M., Hu, X.-J., Wang, X., Liu, S.-H., Jiang, L.-H., 2017. Biochar as potential sustainable precursors for activated carbon production: multiple applications in environmental protection and energy storage. Bioresour. Technol. 227, 359–372.

Tan, X., Zhu, S., Show, P.L., Qi, H., Ho, S.H., 2020. Sorption of ionized dyes on high-salinity microalgal residue derived biochar: electron acceptor-donor and metal-organic bridging mechanisms. J. Hazard. Mater. 393, 122435.

Tang, L., Huang, H., 2005. Plasma pyrolysis of biomass for production of syngas and carbon adsorbent. Energy Fuel 19, 1174–1178.

Tejedor-Sanz, S., Quejigo, J.R., Berná, A., Esteve-Núñez, A., 2017. The planktonic relationship between fluid-like electrodes and bacteria: wiring in motion. Chem. Sus. Chem. 10 (4), 693–700.

Tekin, K., Karagöz, S., Bektaş, S., 2014. A review of hydrothermal biomass processing. Renew. Sust. Energ. Rev. 40, 673–687.

Tiquia-Arashiro, S.M., Pant, D. (Eds.), 2020. Microbial Electrochemical Technologies. CRC Press.

Titirici, M.-M., White, R.J., Falco, C., Sevilla, M., 2012. Black perspectives for a green future: hydrothermal carbons for environment protection and energy storage. Energy Environ. Sci. 5 (5), 6796–6822.

Tong, Y., McNamara, P.J., Mayer, B.K., 2019. Adsorption of organic micropollutants onto biochar: a review of relevant kinetics, mechanisms and equilibrium. Environ. Sci.: Water Res. Technol. 5, 821–838.

Tong, X., Li, J., Yuan, J., Xu, R., 2011. Adsorption of Cu(II) by biochars generated from three crop straws. Chem. Eng. J. 172, 828–834.

Torri, C., Samorì, C., Adamiano, A., Fabbri, D., Faraloni, C., Torzillo, G., 2011. Preliminary investigation on the production of fuels and bio-char from *Chlamydomonas reinhardtii* biomass residue after bio-hydrogen production. Bioresour. Technol. 102 (18), 8707–8713.

Tripathi, M., Sahu, J.N., Ganesan, P., 2016. Effect of process parameters on production of biochar from biomass waste through pyrolysis: a review. Renew. Sust. Energy Rev. 55, 467–481.

Truong, H., Lomnicki, S., Dellinger, B., 2010. Potential for misidentification of environmentally persistent free radicals as molecular pollutants in particulate matter. Environ. Sci. Technol. 44, 1933–1939.

Uchimiya, M., Lima, I.M., Thomas Klasson, K., Chang, S., Wartelle, L.H., Rodgers, J.E., 2010. Immobilization of heavy metal ions (CuII, CdII, NiII, and PbII) by broiler litter derived biochars in water and soil. J. Agric. Food Chem. 58 (9), 5538–5544.

Uchimiya, M., Chang, S., Klasson, K.T., 2011. Screening biochars for heavy metal retention in soil: role of oxygen functional groups. J. Hazard. Mater. 190, 432–441.

Uemura, Y., Matsumoto, R., Saadon, S., Matsumura, Y., 2015. A study on torrefaction of *Laminaria japonica*. Fuel Process. Technol. 138, 133–138.

Van Vinh, N., Zafar, M., Behera, S., Park, H.-S., 2015. Arsenic (III) removal from aqueous solution by raw and zinc-loaded pine cone biochar: equilibrium, kinetics, and thermodynamics studies. Int. J. Environ. Sci. Technol. 12, 1283–1294.

Vaughn, S.F., Kenar, J.A., Thompson, A.R., Peterson, S.C., 2013. Comparison of biochars derived from wood pellets and pelletized wheat straw as replacements for peat in potting substrates. Ind. Crop. Prod. 51, 437–443.

Vijayaraghavan, K., Balasubramanian, R., 2015. Is biosorption suitable for discontamination of metal bearing wastewaters? A critical review on the state-of the-art of biosorption processes and future directions. J. Environ. Manag. 160, 283–296.

Vithanage, M., Rajapaksha, A.U., Zhang, M., Thiele-Bruhn, S., Lee, S.S., Ok, Y.S., 2015. Acid-activated biochar increased sulfamethazine retention in soils. Environ. Sci. Pollut. Res. 22, 2175–2186.

Wan, Y., Chen, P., Zhang, B., Yang, C., Liu, Y., Lin, X., Ruan, R., 2009. Microwave-assisted pyrolysis of biomass: catalysts to improve product selectivity. J. Anal. Appl. Pyrol. 86, 161–167.

Wang, J., Chen, C., 2009. Biosorbents for heavy metals removal and their future. Biotechnol. Adv. 27, 195–226.

Wang, Y., Wang, X.J., Liu, M., Wang, X., Wu, Z., Yang, L.Z., Xia, S.Q., Zhao, J.F., 2012. Cr(VI) removal from water using cobalt-coated bamboo charcoal prepared with microwave heating. Ind. Crop. Prod. 39, 81–88.

Wang, K., Brown, R.C., Homsy, S., Martinez, L., Sidhu, S.S., 2013. Fast pyrolysis of microalgae remnants in a fluidized bed reactor for bio-oil and biochar production. Bioresour. Technol. 127, 494–499.

Wang, H., Gao, B., Wang, S., Fang, J., Xue, Y., Yang, K., 2015a. Removal of Pb(II), Cu(II), and Cd(II) from aqueous solutions by biochar derived from $KMnO_4$ treated hickory wood. Bioresour. Technol. 197, 356–362 2015a.

Wang, S.S., Gao, B., Zimmerman, A.R., Li, Y., Ma, L.C., Harris, W.G., Migliaccio, K.W., 2015b. Removal of arsenic by magnetic biochar prepared from pinewood and natural hematite. Bioresour. Technol. 175, 391–395.

Wang, Y.-Y., Lu, H.-H., Liu, Y.-X., Yang, S.-M., 2016. Removal of phosphate from aqueous solution by SiO_2-biochar nanocomposites prepared by pyrolysis of vermiculite treated algal biomass. RSC Adv. (87).

Wang, S., Gao, B., Li, Y., Creamer, A.E., He, F., 2017. Adsorptive removal of arsenate from aqueous solutions by biochar supported zero-valent Iron nanocomposite: batch and continuous flow tests. J. Hazard. Mater. 322, 172–181.

Wang, Y.-S., Li, D.-B., Zhang, F., Tong, Z.-H., Yu, H.-Q., 2018. Algal biomass derived biochar anode for efficient extracellular electron uptake from *Shewanella oneidensis* MR-1. Front. Environ. Sci. Eng. 12 (4), 11.

Wang, S., Zhou, Y., Han, S., Wang, N., Yin, W., Yin, X., Gao, B., Wang, X., Wang, J., 2018. Carboxymethyl cellulose stabilized ZnO/biochar nanocomposites: enhanced adsorption and inhibited photocatalytic degradation of methylene blue. Chemosphere 197, 20–25.

Wang, H., Wang, H., Zhao, H., Yan, Q., 2020a. Adsorption and Fenton-like removal of chelated nickel from Zn-Ni alloy electroplating wastewater using activated biochar composite derived from Taihu blue algae. Chem. Eng. J. 379, 122372.

Wang, Y., Yang, Q., Chen, J., Yang, J., Zhang, Y., Chen, Y., Li, X., Du, W., Liang, A., Ho, S.H., Chang, J.S., 2020b. Adsorption behavior of Cr(VI) by magnetically modified *Enteromorpha prolifera* based biochar and the toxicity analysis. J. Hazard. Mater. 395, 122658.

Wang, B., Li, Y., Zheng, J., Hu, Y., Wang, X., Hu, B., 2020c. Efficient removal of U(VI) from aqueous solutions using the magnetic biochar derived from the biomass of a bloom-forming cyanobacterium (*Microcystis aeruginosa*). Chemosphere 254, 126898.

Wu, G.-Q., Zhang, X., Hui, H., Yan, J., Zhang, Q.-S., Wan, J.-L., Dai, Y., 2012. Adsorptive removal of aniline from aqueous solution by oxygen plasma irradiated bamboo based activated carbon. Chem. Eng. J. 185, 201–210.

Xiao, L.-P., Shi, Z.-J., Xu, F., Sun, R.-C., 2012. Hydrothermal carbonization of lignocellulosic biomass. Bioresour. Technol. 118, 619–623.

Xiao, X., Agusti, S., Lin, F., Li, K., Pan, Y., Yu, Y., Zheng, Y., Wu, J., Duarte, C.M., 2017. Nutrient removal from Chinese coastal waters by large-scale seaweed aquaculture. Sci. Rep. 7, 46613.

Xiao, X., Chen, B.L., Chen, Z.M., Zhu, L.Z., Schnoor, J.L., 2018. Insight into multiple and multilevel structures of biochars and their potential environmental applications: a critical review. Environ. Sci. Technol. 52, 5027–5047.

Xu, Y., Zheng, X., Yu, H., Hu, X., 2014. Hydrothermal liquefaction of *Chlorella pyrenoidosa* for bio-oil production over Ce/HZSM-5. Bioresour. Technol. 156, 1–5.

Xue, L.H., Gao, B., Wan, Y.S., Fang, J.N., Wang, S.S., Li, Y.C., Munoz-Carpena, R., Yang, L.Z., 2016. High efficiency and selectivity of MgFe-LDH modified wheat-straw biochar in the removal of nitrate from aqueous solutions. J. Taiwan Inst. Chem. E 63, 312–317.

Yang, G.-X., Jiang, H., 2014. Amino modification of biochar for enhanced adsorption of copper ions from synthetic wastewater. Water Res. 48, 396–405.

Yang, K., Xing, B., 2010. Adsorption of organic compounds by carbon nanomaterials in aqueous phase: polanyi theory and its application. Chem. Rev. 110, 5989–6008.

Yang, R., Liu, G., Xu, X., Li, M., Zhang, J., Hao, X., 2011. Surface texture, chemistry and adsorption properties of acid blue 9 of hemp (*Cannabis sativa* L.) bast-based activated carbon fibers prepared by phosphoric acid activation. Biomass Bioenergy 35, 437–445.

Yang, X., Zhang, S., Ju, M., Liu, L., 2019. Preparation and modification of biochar materials and their application in soil remediation. Appl. Sci. 9, 1365.

Yao, Y., Gao, B., Fang, J., Zhang, M., Chen, H., Zhou, Y., Creamer, A.E., Sun, Y., Yang, L., 2014. Characterization and environmental applications of clay-biochar composites. Chem. Eng. J. 242, 136–143.

Yao, Y., Gao, B., Wu, F., Zhang, C.Z., Yang, L.Y., 2015. Engineered biochar from biofuel residue: characterization and its silver removal potential. ACS Appl. Mater. Interfaces 7, 10634–10640.

Yao, Y., Zhang, Y., Gao, B., Chen, R., Wu, F., 2018. Removal of sulfamethoxazole (SMX) and sulfapyridine (SPY) from aqueous solutions by biochars derived from anaerobically digested bagasse. Environ. Sci. Pollut. R. 25, 25659–25667.

Yek, P.N.Y., Peng, W., Wong, C.C., Liew, R.K., Ho, Y.L., Wan Mahari, W.A., Azwar, E., Yuan, T.Q., Tabatabaei, M., Aghbashlo, M., Sonne, C., Lam, S.S., 2020. Engineered biochar via microwave CO_2 and steam pyrolysis to treat carcinogenic Congo red dye. J. Hazard. Mater. 395, 122636.

Yu, G., Zhang, Y., Schideman, L., Funk, T., Wang, Z., 2011. Distributions of carbon and nitrogen in the products from hydrothermal liquefaction of low-lipid microalgae. Energy Environ. Sci. 4 (11), 4587.

Yu, Y., Wang, C., Guo, X., Paul, C.J., 2015. Modification of carbon derived from *Sargassum* sp. by lanthanum for enhanced adsorption of fluoride. J. Colloid Interface Sci. 441, 113–120.

Yu, Z., Zhou, L., Huang, Y., Song, Z., Qiu, W., 2015. Effects of a manganese oxide-modified biochar composite on adsorption of arsenic in red soil. J. Environ. Manag. 163, 155–162.

Yu, K.L., Show, P.L., Ong, H.C., Ling, T.C., Chi-Wei Lan, J., Chen, W.H., 2017a. Microalgae from wastewater treatment to biochar – feedstock preparation and conversion technologies. Energy Convers. Manag. 150, 1–13.

Yu, K.L., Lau, B.F., Show, P.L., Ong, H.C., Ling, T.C., Chen, W.H., Poh, N.E., Chang, J.S., 2017b. Recent developments on algal biochar production and characterization. Bioresour. Technol. 246, 2–11.

Yu, S., Wang, X., Yao, W., Wang, J., Ji, Y., Ai, Y., Alsaedi, A., Hayat, T., Wang, X., 2017c. Macroscopic, spectroscopic, and theoretical investigation for the interaction of phenol and naphthol on reduced graphene oxide. Environ. Sci. Technol. 51 (6), 3278–3286.

Yu, K.L., Lee, X.J., Ong, H.C., Chen, W.H., Chang, J.S., Lin, C.S., Show, P.L., Ling, T.C., 2020. Adsorptive removal of cationic methylene blue and anionic Congo red dyes using wet-torrefied microalgal biochar: equilibrium, kinetic and mechanism modelling. Environ. Pollut. https://doi.org/10.1016/j.envpol.2020.115986.

Yuan, Y., Zhou, S., Liu, Y., Tang, J., 2013. Nanostructured macroporous bioanode based on polyaniline-modified natural loofah sponge for high-performance microbial fuel cells. Environ. Sci. Technol. 47 (24), 14525–14532.

Yuan, H., Deng, L., Qi, Y., Kobayashi, N., Tang, J., 2014. Nonactivated and activated biochar derived from bananas as alternative cathode catalyst in microbial fuel cells. Sci. World J. 2014, 8.

Yuan, Y., Bolan, N., Prévoteau, A., Vithanage, M., Biswas, J.K., Ok, Y.S., Wang, H., 2017. Applications of biochar in redox-mediated reactions. Bioresour. Technol. 246, 271–281.

Zhang, M., Gao, B., 2013. Removal of arsenic, methylene blue, and phosphate by biochar/AlOOH nanocomposite. Chem. Eng. J. 226, 286–292.

Zhang, S., Xiong, Y., 2016. Washing pretreatment with light bio-oil and its effect on pyrolysis products of bio-oil and biochar. RSC Adv. 6 (7), 5270–5277.

Zhang, M., Gao, B., Varnoosfaderani, S., Hebard, A., Yao, Y., Inyang, M., 2013. Preparation and characterization of a novel magnetic biochar for arsenic removal. Bioresour. Technol. 130, 457–462.

Zhang, W., Zheng, J., Zheng, P., Qiu, R., 2015. Atrazine immobilization on sludge derived biochar and the interactive influence of coexisting Pb(II) or Cr(VI) ions. Chemosphere 134, 438–445.

Zhang, C., Ho, S.-H., Chen, W.-H., Xie, Y., Liu, Z., Chang, J.-S., 2018. Torrefaction performance and energy usage of biomass wastes and their correlations with torrefaction severity index. Appl. Energy 220, 598–604.

Zhang, C., Lu, J., Wu, J., 2020. One-step green preparation of magnetic seaweed biochar/sulfidated Fe_0 composite with strengthen adsorptive removal of tetrabromobisphenol A through in situ reduction. Bioresour. Technol. 307, 123170.

Zhao, L., Cao, X., Masek, O., Zimmerman, A., 2013. Heterogeneity of biochar properties as a function of feedstock sources and production temperatures. J. Hazard. Mater. 256–257, 1–9.

Zhao, Y.-Q., Lu, M., Tao, P.-Y., Zhang, Y.-J., Gong, X.-T., Yang, Z., Zhang, G.-Q., Li, H.-L., 2016. Hierarchically porous and heteroatom doped carbon derived from tobacco rods for supercapacitors. J. Power Sour. 307, 391–400.

Zheng, H., Guo, W., Li, S., Chen, Y., Wu, Q., Feng, X., Yin, R., Ho, S.H., Ren, N., Chang, J.S., 2017. Adsorption of p-nitrophenols (pnp) on microalgal biochar: analysis of high adsorption capacity and mechanism. Bioresour. Technol. 244, 1456–1464.

Zhou, Y., Gao, B., Zimmerman, A.R., Chen, H., Zhang, M., Cao, X., 2014. Biochar-supported zerovalent iron for removal of various contaminants from aqueous solutions. Bioresour. Technol. 152, 538–542.

Zhou, Y.Y., Liu, X.C., Xiang, Y.J., Wang, P., Zhang, J.C., Zhang, F.F., Wei, J.H., Luo, L., Lei, M., Tang, L., 2017. Modification of biochar derived from sawdust and its application in removal of tetracycline and copper from aqueous solution: adsorption mechanism and modelling. Bioresour. Technol. 245 (Pt A), 266–273.

Zhou, Y., Zhang, H., Cai, L., Guo, J., Wang, Y., Ji, L., Song, W., 2018. Preparation and characterization of macroalgae biochar nanomaterials with highly efficient adsorption and photodegradation ability. Mater. 11, 1709 2018.

Zhu, X., Chen, B., Zhu, L., Xing, B., 2017. Effects and mechanisms of biochar-microbe interactions in soil improvement and pollution remediation: a review. Environ. Pollut. 227, 98–115.

Zhu, X., Li, C., Li, J., Xie, B., Lv, J., Li, Y., 2018. Thermal treatment of biochar in the air/nitrogen atmosphere for developed mesoporosity and enhanced adsorption to tetracycline. Bioresour. Technol. 263, 475–482.

Zimmerman, A.R., 2010. Abiotic and microbial oxidation of laboratory-produced lack carbon (biochar). Environ. Sci. Technol. 44, 1295–1301.